University of South Carolina
Scholar Commons

Theses and Dissertations

Fall 2019

Heterogeneous Ozonation of Model Drinking Water Contaminants Using CBV-720 ZEOLITE

Benson Maxwell Solomon

Follow this and additional works at: https://scholarcommons.sc.edu/etd

 Part of the Chemistry Commons

Recommended Citation

Solomon, B. M.(2019). *Heterogeneous Ozonation of Model Drinking Water Contaminants Using CBV-720 ZEOLITE.* (Doctoral dissertation). Retrieved from https://scholarcommons.sc.edu/etd/5577

This Open Access Dissertation is brought to you by Scholar Commons. It has been accepted for inclusion in Theses and Dissertations by an authorized administrator of Scholar Commons. For more information, please contact dillarda@mailbox.sc.edu.

HETEROGENEOUS OZONATION OF MODEL DRINKING WATER CONTAMINANTS USING CBV-720 ZEOLITE

by

Benson Maxwell Solomon

Bachelor of Science
High Point University, 2012

Submitted in Partial Fulfillment of the Requirements

For the Degree of Doctor of Philosophy in

Chemistry

College of Arts and Sciences

University of South Carolina

2019

Accepted by:

John Ferry, Major Professor

S. Michael Angel, Committee Member

Chuanbing Tang, Committee Member

Jamie Lead, Committee Member

Cheryl L. Addy, Vice Provost and Dean of the Graduate School

© Copyright by Benson Solomon, 2019
All Rights Reserved.

DEDICATION

To my wife Jesie, thank you so much for your support and patience throughout our college years. I can't wait to see where our next adventure will unfold.

I would also like to dedicate this work to my grandfather, Dr. Herbert M Solomon, or to his grandchildren, Popop. I only wish he could be here to see me graduate and we could play one last round of golf.

ACKNOWLEDGEMENTS

I must thank my advisor Dr. John Ferry for his seemingly endless patience and guidance throughout my time at USC. Without his encouragement and knowledge, I certainly wouldn't be where I am today. I would also like to thank my PhD committee, Dr. Mike Angel, Dr. Chuanbing Tang, and Dr. Jamie Lead.

I want to thank several of my fellow graduate students who have become great friends as we prepared for seminars, defenses, teaching assignments, and research. From the Ferry group: Dr. Sarah Murphy, Dr. Joy Ihekweazu, Dr. Shengnan Meng, Meagan Smith, Fan Wang, and Sam Putnam. From the Shaw group: Dr. Justin Copeland and Dr. Muditha Dias.

Finally, I want to thank several friends and mentors from High Point University that always supported and encouraged me to become a scientist: Dr. Gray Bowman, Dr. Christopher Fowler, Dr. Elizabeth McCorquodale, Dr. Aaron Titus, Dr. Todd Knippenberg (even though he went to Clemson), and Dr. Harold Goldston.

ABSTRACT

Advanced Oxidation Processes (AOPs) are designed to remove aqueous organic contaminants through their reaction with hydroxyl radicals (HO·). Ozone is classified as an AOP due to its ability to produce hydroxyl radicals, as well as its ability to oxidize a wide range of organic contaminants. Due to the unselective nature of hydroxyl radicals, many organic and inorganic co-solutes can act as scavengers, reducing the efficiency of an AOP. Here we show a probe system for testing the hypothesis that adsorptive ozonation of contaminants may yield a more selective environment that favors neutral contaminant oxidation over oxidation of co-solutes.

Initial experiments examined the hydroxyl radical probe 3-nitro-α α, α,-trifluorotoluene (TFNT) at pH 7.8 during continuous ozone exposure with varying amounts of CBV 720 (SiO_2:Al_2O_3 = 30, unit cell 24.3 and surface area = 780 m^2/gram) zeolite with 0.05 wt% resulting in the fastest oxidation rates. Baseline results were obtained by observing the oxidation rate of TFNT in the presence and absence of a 0.05 wt% zeolite suspension. In the interest of higher sample throughput, a dosed ozone reaction system was developed. Inside this system, experiments investigated the behavior of HO· and its affinity for TFNT adsorbed to the zeolite. Addition of the radical scavenger bicarbonate ion decreased TFNT oxidation rates in solution, consistent with the effect of a negatively charged surface repelling carbonate from the local environment of the reaction, as well as the ability of carbonate to effectively scavenge HO·. A second

HO· scavenger, dichloroacetic acid (DCAA), was added which would not adsorb to the zeolite but remained in solution. This allowed an investigation into the behavior of HO· in the presence of a scavenger adsorbed to zeolite and a scavenger in solution.

Oxidation rates were not increased by the addition of zeolite during ozonation. The zeolite demonstrated the ability to sequester TFNT on its surface, making it harder for HO· to react and decreasing oxidation rates while having little to no effect on DCAA oxidation. Despite the inhibition of TFNT oxidation, the process was not stopped completely and TFNT was still mostly removed

TABLE OF CONTENTS

LIST OF TABLES

LIST OF FIGURES

LIST OF SYMBOLS

R_{ct}	Ratio of the concentration of hydroxyl radical to the concentration of ozone.
$X_{y/z}$	Fraction of y scavenged by z
Q	Maximum adsorbate that can be adsorbed to a surface
b	Lagmuir isotherm constant
pH_{PZC}	pH when the surface charge is 0

LIST OF ABBREVIATIONS

AOP..... Advanced Oxidation Process

DCAA ..... Dichloroacetic acid

H_2O_2 ..... Hydrogen Peroxide

HO·..... Hydroxyl Radical

$\cdot O_2^-$ ..... Superoxide

O_3 ..... Ozone

ROS.....Reactive Oxygen Species

TFNT.....3-nitro-α, α, α-trifluorotoluene

UV.....Ultraviolet Light

CHAPTER 1

1.1 Introduction

According to the World Resources Institute, the world's demand for clean water for consumption, farming, and industrialization, will increase greatly over the next few decades due to a rapidly growing world population.[1] Approximately 1 billion people live in an area where the water supply is considered stressed and it is estimated that half the world's population could experience a decrease in water availability by 2025. A stressed water supply is defined as when the ratio of water withdrawal to supply is greater than 40-50%. In the United States, it is expected that the need for clean water will increase by as much as 25% by 2050.[2] Communities will increasingly face challenges to their water supply from continued population growth, climate change, and wastewater effluent due to the 32 billion gallons of treated wastewater discharged into surface waters each day in the United States.[3] While the use of groundwater (water naturally stored underground) can supplement the availability of water to communities, there are some major problems that must be addressed. Water treatment technologies must be improved due to the presence of many constituents that may render the water unusable for some applications, the most important being human consumption; before water reuse and groundwater are to become relied upon as a significant water source.

As of 2013, it is estimated that water reuse for applications such as industry, irrigation, and potable water only accounts for up to 1% of water use, although this estimate is likely to be low.[3] 20% of the national water withdrawal came from ground

water sources.[4] As groundwater becomes a more relied upon source of water, the US must monitor the quality of the groundwater that has been subject to the release of anthropogenic chemicals as a byproduct of an industrialized nation. The Groundwater Foundation estimates that over half the United States population relies on groundwater for most of its water supply, including 99% of the rural population with ~27 trillion gallons of groundwater being withdrawn for use each year.[5] Since its inception, the Environmental Protection Agency (EPA) has been leading the way (in conjunction with the United States Geological Survey) in monitoring and restoration of surface and groundwater. The waste discharged into wastewater systems encompass a wide variety of biological, inorganic, and organic contaminants; each need to be investigated and treated as necessary, and every treatment technology of these waters has both beneficial and detrimental consequences to each respective treatment.

As of 2003, the EPA has identified over 300,000 sites that need remediation to make the water suitable for use as a water source. Cost estimates to complete this remediation show an investment of over $200 billion will be required.[6] This is likely an underestimate because sites that are currently undergoing remediation do not count toward the total, and assumes no more waste sites will be identified in the future. Of those 300,000 sites, 120,000 of them have soil or water contamination that makes the groundwater unsafe for consumption, and approximately 10% of them are believed to threaten a public water supply. Many of the organic contaminants are low solubility (<10 ppm), hydrophobic organic molecules with concentrations at saturation in the environment on the micromolar level or below. Tetrachloroethylene is an example of a persistent contaminant in groundwater which was once a widely used industrial solvent

and dry-cleaning agent; and has become a common soil and groundwater contaminant subject to significant remediation research. A report to the World Health Organization estimated that, in the United States in 1981, 350,000 tons of TCE where produced and decreased to 169,000 by the mid-1990s due to increased government regulations and improved technology.[7] An estimated 1300 tons of TCE where released by manufacturing facilities in 2002 alone. In addition, estimates are that 80-85% of TCE used annually is released into the atmosphere. Estimates for the half-life of TCE in the atmosphere vary widely depending on the removal process. While the lifetime of TCE was thought to be around 3 months due to the reaction with chlorine atoms and hydroxyl radicals, it could be as long as 3 years for gas-phase photolysis.[7] In 2008, it was reported that the Anniston Army Depot in Alabama had groundwater contaminated with an estimated 27 million pounds of TCE, in addition to other solvents and metals[6]. These contaminants were believed to be migrating away from the source and threatening the water supply of Anniston, Alabama. Remediation efforts, mainly consisting of air striping and activated carbon filtration, have lowered TCE levels in extracted water below drinking water standards (<5 parts per billion); however, due to the extent of contamination, estimated timelines when TCE in groundwater would be below drinking water standards is in the hundreds to thousands of years.

There are many technologies that allow for the remediation of contaminated water and groundwater through the use of physical, biological, and chemical processes. Physical removal typically involves the removal and isolation of contaminated solids from water with possible incineration of the resulting sludge. The sludge must be dewatered to >25% dry solids before being heated to over 800°C.[8] While this can be

effective for small, contained contaminations, it is logistically difficult and expensive for large spills that may penetrate deep beneath the surface. In addition, the production of byproducts such as dioxins, furans, nitrogen oxides (NO_x), and sulfur dioxide (SO_2) have been linked to incineration [2, 9, 10].

Biological remediation utilizes native bacteria and microorganisms capable of the removal of a given contaminant. This natural attenuation is often slow and requires frequent management. Figure 1.1 demonstrates a schematic of the bioremediation process.

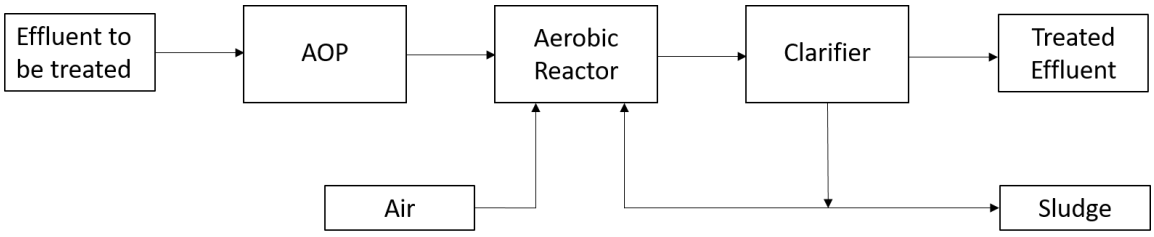

Figure 1.1 Water treatment scheme using an AOP with biological treatment.[11]

A contaminated mixture is usually first treated with an advanced oxidation process before being moved to an aerobic reactor to increase bacterial growth. Mixtures of chlorinated hydrocarbons such as tetrachloroethylene and trichloroethylene have been successfully bioremediated under anaerobic conditions by reductive dechlorination by *Dehalococcoides sp.* and under aerobic conditions by co-metabolism by *Pseudomonas sp.*[12, 13] Partial degradation products of tetrachloroethylene from these two microorganisms include trichloroethylene and vinyl chloride with final products being ethane and HCl.

The application of chemical technologies uses strong chemical oxidants such as hypochlorous acid, chlorine dioxide, chloramine, ozone, and hydrogen peroxide with the goal of the complete mineralization of contaminants. It is also common to combine different remediation techniques to allow a more complete (organics $\rightarrow CO_2+H_2O$) treatment of water.

While physical, biological, and chemical processes are interesting and useful strategies for the removal of organic contaminants, all have limitations. Given the wide variety of structures and properties included under the term 'contaminants,' a general-purpose technology must rely on non-selective species capable of reacting with wide classes of molecules found in water (e.g. aromatics, aliphatics, etc.). Examination of the highly reactive species generated by the interaction of relativistic particles with aqueous solutions provides a roadmap of the highest-energy species available as possible reagents in water.

The interaction of beams of high energy electrons with aqueous solutions will fragment incident waters according to equations 1 and 2, and lead to a series of radical reactions:

$$H_2O \xrightarrow{185\ nm} HO\cdot + H\cdot \quad \Phi=0.3 \qquad [1]$$

$$H_2O \xrightarrow{185\ nm} HO\cdot + H^+ + e_{aq}^- \quad \Phi=0.045 \qquad [2]$$

$$HO_2\cdot \leftrightarrow \cdot O_2^- + H^+ \qquad [3]$$

$$\cdot O_2^- + HO\cdot \rightarrow O_2 + OH^- \qquad [4]$$

$$HO_2\cdot + HO\cdot \rightarrow H_2O + O_2 \qquad [5]$$

$$e_{aq}^- + O_2 \rightarrow \cdot O_2^- \qquad [6]$$

$$e_{aq}^- + H\cdot + H_2O \rightarrow H_2 + OH^- \qquad [7]$$

$$e_{aq}^{-} + HO \cdot \rightarrow OH^{-} \quad [8]$$

The source of high energy radiation can come from radioactive isotopes producing α, β, and γ radiation, or from low pressure mercury lamps capable of producing 185 nm light with a quartz envelope to absorb 254 nm light. Buxton et al.[14] summarized the reactions with the first (equations 1 and 2) being the hemolysis of water and the second being the ionization of water. Radiolysis of water produces many different radical and oxidative species, organized in order of decreasing reduction potential: HO· (2.72 V), H_2O_2 (1.77V), $\cdot O_2^-$(0.36V), H_2 (-0.42V), H· (-2.1V), and hydrated electrons (e^-_{aq}) (-2.7V). An immediate advantage of this kind of technology is that there are no reagents required to add to a contaminated solution making it more environmentally friendly.

Advanced Oxidation Processes (AOPs) are widely used in water treatment due to their ability to produce oxidizing radicals such as the hydroxyl radical (HO·). These processes are particularly useful for removing biologically toxic and relatively stable materials such as pesticides, aromatics, and volatile organic compounds. Hydroxyl radical is a strong oxidant (E^o = 2.72 V vs NHE)[15] that has bimolecular rate constants for most organics with values ranging between 10^8-10^{10} M^{-1} s^{-1}.[16] There are several different AOPs (*hv*/H_2O, H_2O_2/Fe^{2+}, H_2O_2/UV, O_3/H_2O_2, O_3/UV), and they all have the production of HO· in common.[17] HO· is the strongest oxidant kinetically stable in water. It is capable of reacting with organic contaminants through three known mechanisms: hydrogen abstraction, particularly from saturated carbon (reaction #9); electrophilic addition to aromatic rings or unsaturated carbon (reaction #10); and electron transfer without bond formation (reaction #11).[18]

$$HO\cdot + RH \rightarrow R\cdot + H_2O \quad [9]$$

$$HO\cdot + PhX \rightarrow HOPhX\cdot \quad [10]$$

$$HO\cdot + RX \rightarrow \cdot RX^+ + OH^- \quad [11]$$

Hydrogen abstraction is straightforward when HO· reacts with alkanes. When HO· reacts with methane, HO· removes an H and gives a methyl radical.

$$HO\cdot + CH_4 \rightarrow HOH + \cdot CH_3 \quad [12]$$

Electrophilic addition of HO· to tetrachloroethylene yields the HO-tetrachloroethyl radical (equation 5) where HO· adds to one of the carbon molecules.

$$HO\cdot + C_2Cl_4 \rightarrow HOC_2Cl_4\cdot \quad [13]$$

The reaction of HO· with an organic molecule through electron transfer is believed to be less common and can be demonstrated by its reaction with Fe(II)EDTA. The resulting products are Fe(III)EDTA and OH^-.

$$HO\cdot + Fe(II)EDTA \rightarrow Fe(III)EDTA + OH^- \quad [14]$$

One major limitation to HO· producing technologies are the intrinsic reactivity of HO· with itself (reaction 15), also called dismutation. Due to its self-reaction rate of ~5.5×10^9 M^{-1} s^{-1} [14], it is effectively impossible to achieve concentrations greater than 10^{-12} M.

$$HO\cdot + HO\cdot \rightarrow H_2O_2 \quad [15]$$

AOP reactions have been observed occurring naturally in varying environments in the presence sunlight where ROS production is initiated through the photoreduction of Fe^{III} to Fe^{II}. Murphy et al.[19](Appendix A) showed that this process can occur during nighttime conditions where microbially produced hydrogen sulfide species drive the production of Fe^{II} from the reduction of Fe^{III} rich sediments. Laboratory experiments were able to replicate the reactions and model the production of hydrogen peroxide at

concentrations observed in the environment. A follow-up paper by Murphy et al.[20] (Appendix B) included the measurement of superoxide and its role in the production of hydrogen peroxide. At a pH of 8.25 the dismutation of superoxide alone accounted for the hydrogen peroxide formation, however at 7.0, dismutation overestimated the hydrogen peroxide production. The authors believed the reaction of hydrogen peroxide with iron and sulfide species accounted for the reduced amount of hydrogen peroxide observed.

Due to the constraints demonstrated by the dismutation of HO·, synthesis techniques are required capable of rapid production of HO· to achieve the highest possible concentrations in solution.

After HO·, the next most reactive molecular species generated in these processes is the hydrogen atom. While HO· is the most powerful oxidant kinetically stable in water, the hydrogen atom is the most powerful reductant (E^0=-2.3 V), capable of multiple different reactions with organic matter such as: the reduction of functional groups such as alkenes, hydrogen abstraction, or one electron transfer.

The reduction of ethene (C_2H_4), by H· demonstrates the reduction of an alkene by H· (equation 16) where the H· adds to one of the carbons resulting in a carbon radical.

$$H\cdot + C_2H_4 \rightarrow \cdot C_2H_5 \qquad [16]$$

Hydrogen abstraction of acetic acid by H· demonstrates how H· can remove an H atom resulting in the creation H_2 and another carbon radical.

$$H\cdot + CH_3COOH \rightarrow \cdot CH_2COOH + H_2 \qquad [17]$$

The one electron transfer of H· to tetranitromethane ($C(NO_2)_4$) demonstrates how H· can reduce an organic molecule by one electron resulting in the trinitromethane anion, H+, and a nitrite radical.

$$H\cdot + C(NO_2)_4 \rightarrow C(NO_2)_3^- + H^+ + \cdot NO_2 \quad [18]$$

Like HO·, self-reactions limit the maximum concentrations of H· (~10^{-14} M) with a rate of ~5x10^9 M^{-1} s^{-1}.

$$H\cdot + H\cdot \rightarrow H_2 \quad [19]$$

However, unlike HO·, H· is also reactive with common molecules found in water that can further reduce its concentration. Molecular oxygen is typically found in surface water concentrations of 250 µM or higher and is capable of reacting with H· (equation 20) with a rate of 1x10^{10} M^{-1} s^{-1}.

$$H\cdot + O_2 \rightarrow HO_2\cdot \quad [20]$$

The universal presence of molecular oxygen in surface and groundwater therefore reduces the maximum concentration of H· to concentrations lower than HO· can achieve. While the resulting HO_2· radical is itself a strong oxidant with a reduction potential of 1.06 V, it is significantly weaker than HO· (2.72 V).

The hydrated electron is a strong reductant (E^0=-2.9 V), capable of enhanced reactions when organics contain electron withdrawing groups; such as the removal of halogens from halogenated hydrocarbons (equation 21).

$$e_{aq}^- + RX \rightarrow RX^- \rightarrow R\cdot + X^- \quad [21]$$

Superoxide ($\cdot O_2^-$) is a moderately strong reductant (E^0= -0.33 V) with a wide range of rate constants, the highest being around 10^7 with organics. Its conjugate acid hydroperoxyl radical (HO_2·) is a mild oxidant (E^0= 0.05 V). Neither superoxide nor hydroperoxyl radical are as reactive as HO· but can be very reactive towards organic radicals.

Water has a calculated molar extinction coefficient at 185 nm of 0.032 m^{-1} cm^{-1} and approximately 90% of photons are absorbed in the first 5.5 nm of water which is

much shorter than the distance 254 nm light can travel.[21] The production of HO· from this process is highly dependent on the power of the lamp, reactor setup, and solvent makeup. Kutschera et al.[22] were able to quantify the hydroxyl radical formation rate to be $1.4x10^{-9}$ M for 1 J/m^2; however, it was unclear what the exact conditions were for this measurement. Rauf and Ashraf[23] published an in depth study of the use of high energy irradiation of water to degrade synthetic dyes commonly found in wastewater. Their data showed that degradation of dyes was due only to the reaction with HO·, and other radicals may react with other intermediate products. They went on to describe a pilot plant in South Korea that uses an electron accelerator to produce 1000 L day^{-1} using an electron accelerator in combination with biological treatment. The plant showed such promising results indicating decreased chemical and biological oxygen demand that an industrial plant was completed in 2005 capable of an output of 10,000 L day^{-1} using a 1 MeV, 400 kW accelerator.

Radiolysis is quite useful for introducing the fundamentals of reactive oxygen species chemistry. It demonstrates how and why HO· is the most desired oxidative species in the water treatment process; however, there are multiple AOPs capable of generating HO·, briefly mentioned before: $h\nu/H_2O$, H_2O_2/Fe^{2+}, H_2O_2/UV, O_3/H_2O_2, O_3/UV. Each process is able to generate multiple different oxidative species as shown in table 1.1 with an in-depth discussion of each process to follow.

AOP	Oxidative Species					
	O_3	**O_2**	**$\cdot O_2^-$**	**$HO_2\cdot$**	**$HO\cdot$**	**HO^-**
hv/H_2O		X	X		X	X
H_2O_2/UV		X		X	X	X
H_2O_2/Fe^{2+}		X	X	X	X	X
O_3/H_2O_2	X	X	X	X	X	X
O_3/UV	X	X	X	X	X	X

Table 1.1. This table shows a summary of selected oxidative species produced during each AOP

H_2O_2 photolysis is a method capable of using UV light below 280nm to initiate the homolytic cleavage of H_2O_2 to produce 2 HO·.[17] This method to generate HO· has been known since at least 1957 when Baxendale and Wilson[24] were able to measure the quantum yield during photolysis using 253 nm light.

$$H_2O_2 + hv \rightarrow 2HO\cdot \quad [23]$$

The addition of H_2O_2 significantly decreases the dose of light needed to oxidize contaminants compared to photolysis alone. This reaction is pH sensitive and is more effective under more basic conditions due to HO_2^- having a higher extinction coefficient than H_2O_2 (240 M^{-1} cm^{-1} and 20 M^{-1} cm^{-1} respectively at 253 nm)[11]. Once HO· formation initiates, radical propagation begins (equations 24-26), until termination (equations 27 and 28):

$$HO\cdot + H_2O_2 \rightarrow HO_2\cdot + H_2O \quad [24]$$

$$HO_2\cdot + H_2O_2 \rightarrow HO\cdot + H_2O + O_2 \quad [25]$$

$$HO_2\cdot + HO_2^- \rightarrow HO\cdot + HO^- + O_2 \quad [26]$$

$$HO\cdot + HO_2\cdot \rightarrow H_2O + O_2 \quad [27]$$

$$HO\cdot + HO\cdot \rightarrow H_2O_2 + O_2 \quad [28]$$

H_2O_2 can also react with HO· as seen in equation 24, allowing for the production of more H_2O_2 after the formation of the hydroperoxyl radical (HO_2·). The molar extinction coefficient of H_2O_2 is small, 18.6 M^{-1} cm^{-1} at 254 nm. This becomes a problem in solutions with organic substrates capable of preventing light from reaching the H_2O_2. Stirring the bulk solution continuously places H_2O_2 in contact with light to counter the absorption of light by other constituents. In a complex mixture, reflection, refraction, shadowing, and the lamp itself can greatly influence the distribution of photons capable of degrading H_2O_2. Advantages of H_2O_2 photolysis include the need for addition of only one reagent which is readily available, safe for use, and degrades into water and oxygen. Rosenfeldt et al.[25] showed that H_2O_2 photolysis was more effective at the degradation of endocrine disrupting chemicals such as ethinyl estradiol and bisphenol A than UV treatment alone and they were able to model their degradation in laboratory and natural waters. Endocrine disrupting chemicals are the cause of many adverse effects on humans and animals, manifesting in different reproductive and sexual disabilities, cancer, birth defects, and developmental disorders. One of the more famous examples being the case of the pesticide DDT (dichlorodiphenyltrichloroethane) which was used worldwide to control malaria carrying insects. In 1997, Lundholm[26] published data describing how DDE (dichlorodiphenyldichloroethylene), a common degradation product of DDT, was contributing to the thinning of eggshells of predatory birds. Because of this thinning, the birds would break the eggs when sitting on them. Later discoveries showed that DDT was bioaccumulating in animals all over the world.

The use of transition metals to catalyze the decomposition of H_2O_2 and produce HO· is known as the Fenton reaction, although this most often refers to the use of iron. This reaction (equation 29) has been known for well over a century when it was discovered by Henry John Horstman Fenton as a reagent to test for the presence of tartaric acid.[27] It was not until the 1960s that Fenton's reagents application for water treatment was realized. The mixture of Fe^{2+} and H_2O_2 initiates a complex series of reactions that produce several different oxy radical species capable of reacting with organic and inorganic compounds[28].

Initiation

$$Fe^{2+} + H_2O_2 \rightarrow OH^- + HO\cdot + Fe^{3+} \quad [29]$$

$$Fe^{2+} + O_2 \leftrightarrow Fe^{3+} + \cdot O_2^- \quad [30]$$

Propagation

$$HO_2\cdot \leftrightarrow H^+ + \cdot O_2^- \quad [31]$$

$$Fe^{2+} + HO\cdot \leftrightarrow HO^- + Fe^{3+} \quad [32]$$

$$Fe^{3+} + H_2O_2 \rightarrow FeOOH^{2+} + H^+ \quad [33]$$

$$FeOOH^{2+} \rightarrow HO_2\cdot + Fe^{2+} \quad [34]$$

$$\cdot O_2^- + H_2O_2 \rightarrow OH^- + HO\cdot + O_2 \quad [35]$$

$$HO\cdot + H_2O_2 \rightarrow H_2O + HO_2\cdot \quad [36]$$

Termination

$$HO_2\cdot + HO_2\cdot \rightarrow H_2O_2 + O_2 \quad [37]$$

$$\cdot O_2^- + \cdot O_2^- \xrightarrow{2H^+} Fe^{3+} + H_2O_2 \quad [38]$$

$$\cdot O_2^- + HO_2\cdot \rightarrow H_2O_2 + O_2 \quad [39]$$

$$HO\cdot + HO\cdot \rightarrow H_2O_2 \quad [40]$$

$$Fe^{3+} + H_2O_2 \rightarrow Fe - OOH^{2+} + H^+ \quad [41]$$

$$Fe^{2+} + HO_2 \cdot \rightarrow Fe^{3+} + HO_2^- \quad [42]$$

$$Fe^{3+} + HO_2 \cdot \rightarrow Fe^{2+} + O_2 + H^+ \quad [43]$$

Figure 1.2 graphically shows the iron cycle. Fe^{3+} can be reduced to Fe^{2+} by a reductant such as superoxide. Once reduced, Fe^{2+} will quickly oxide through the reaction with oxygen creating more superoxide or it can react with anther oxidized species capable of producing a multitude of ROS and other radical species.

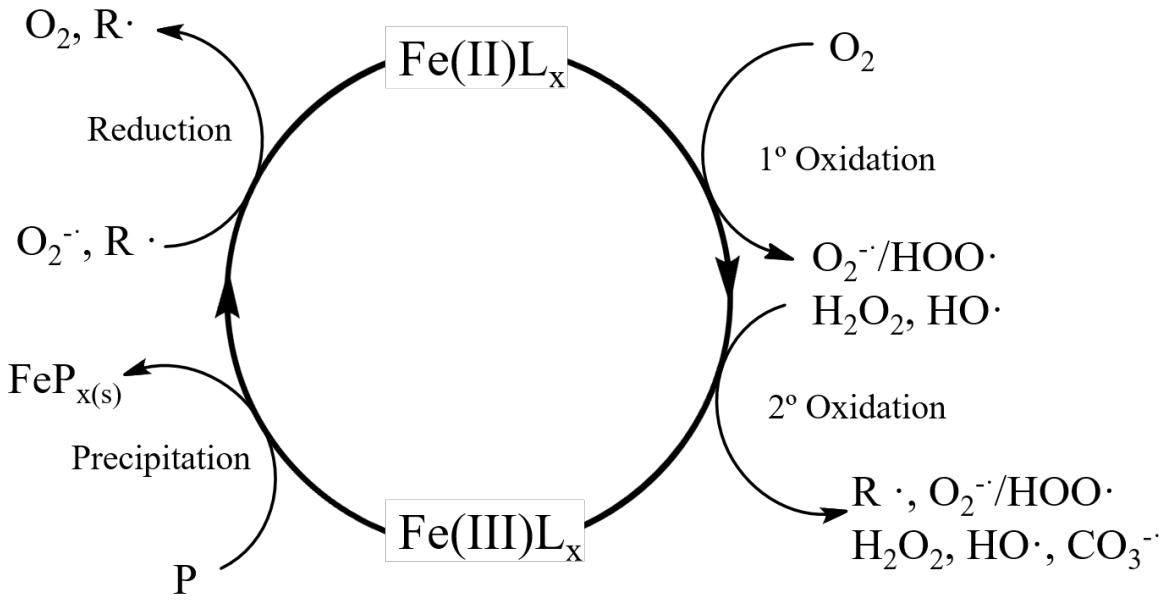

Figure 1.2 Iron cycling between the +2 and +3 oxidation state while generating a suite of ROS. (L= ligand that forms a soluble complex, P= precipitating ligand)[29]

The Fenton reaction has several advantages when applied to water treatment applications. By using iron and hydrogen peroxide, both relatively inexpensive and environmentally friendly, the Fenton reaction has proven to be a safe and effective remediation technology with a greatly increasing amount of research in the last 20 years. The effectiveness of the Fenton reaction can be strongly increased by irradiation with ultraviolet light capable of degrading H_2O_2 and reducing Fe^{3+} to Fe^{2+}, called the photo-Fenton reaction. [30] Some research has also included the use of the Fenton reaction on heterogeneous iron catalysts in support of degrading contaminants in soil and groundwater. Drawbacks from Fenton processes include a strict dependence on pH and the possibility of the production of iron sludges.[17] From a drinking water treatment

standpoint, this method requires a secondary oxidant to maintain the equality of the water after it leaves the treatment facility. Once the H_2O_2 is consumed, the production of oxidants stops, allowing the bacterial growth to occur.

Ozone AOPs are increasingly being used during water treatment due to a few advantages, the first being ozone itself is a disinfectant and strong oxidant (2.07 V)[31] capable of oxidizing more organic matter than other oxidants such as hypochlorous acid (1.60 V) and chlorine dioxide (1.15 V)[32]. Ozone degradation can lead to the production of HO·, and it produces fewer halogenated disinfection by-products. Finally, ozone helps control taste and odor, oxidizes reduced metals, aids coagulation-flocculation. The instability of aqueous O_3 leads to the production of a suite of Reactive Oxygen Species (ROS) such as hydroxyl radical (HO·), superoxide ($\cdot O_2^-$), and hydrogen peroxide (H_2O_2), all of which can react with O_3 and continue the radical chain reactions. Ozone has been a very beneficial molecule within the AOP community for its use as a source of HO·, particularly in conjunction with UV or added reductants like hydrogen peroxide.

The mechanism of ozone decomposition in aqueous solutions is thought to be well understood. UV light can be used in conjunction with O_3 due to the high extinction coefficient of O_3 (3600 M^{-1} cm^{-1}) at 254 nm to increase the degradation of O_3. The reaction of O_3 with UV light produces HO· (equation 44), and two moles of HO· can react to form H_2O_2 (equation 45). The reaction stoichiometry is 1 mole of HO· formed for 1.5 moles of ozone, 0.5 moles of UV photons, and 0.5 moles of H_2O_2.[33] H_2O_2 can then undergo photolysis as mentioned previously in equation 23 or it can react with ozone as described below in equations 44 and 45.

$$O_3 + H_2O \xrightarrow{hv} HO\cdot + O_2 \quad [44]$$

$$2HO\cdot \rightarrow H_2O_2 \quad [45]$$

The O_3/UV process is an effective one used to treat multiple types of organic contaminants. Chen et al.[34] demonstrated that this system was capable of treating nitrotoluene byproducts produced as waste from the manufacture of dyes, pharmaceuticals, and TNT. They showed that the use of O_3 combined with UV light produced a 94% reduction in total organic carbon, resulting in a 76% increase over O_3 alone.

Staehelin and Hoigné[35] showed that the lifetime of ozone decreased as pH increased without the need for UV photons, according to the mechanism:

$$O_3 + OH^- \rightarrow HO_2^- + O_2 \quad [46]$$

$$HO_2^- + O_3 \rightarrow HO_2\cdot + \cdot O_3^- \quad [47]$$

$$HO\cdot_2 \rightleftarrows \cdot O_2^- + H^+ \quad [48]$$

$$\cdot O_2^- + O_3 \rightarrow \cdot O_3^- + O_2 \quad [49]$$

$$\cdot O_3^- + H_2O \rightarrow HO_3 + HO^- \quad [50]$$

$$HO_3 \rightarrow HO\cdot + O_2 \quad [51]$$

Figure 1.3 graphically shows the degradation of ozone and the resulting production of ROS. Oxygen atom transfer from ozone to hydroxide ion to give the conjugate base of hydrogen peroxide, HO_2^-, initiates this family of reactions. Hydroperoxide can in turn donate an electron to a second ozone to generate ozonide and $HO_2\cdot$. $HO_2\cdot$ can dissociate into superoxide, which can also donate an electron to ozone to yield another ozonide. Ozonide is a strong base that protonates in water to yield the unstable HO_3, which

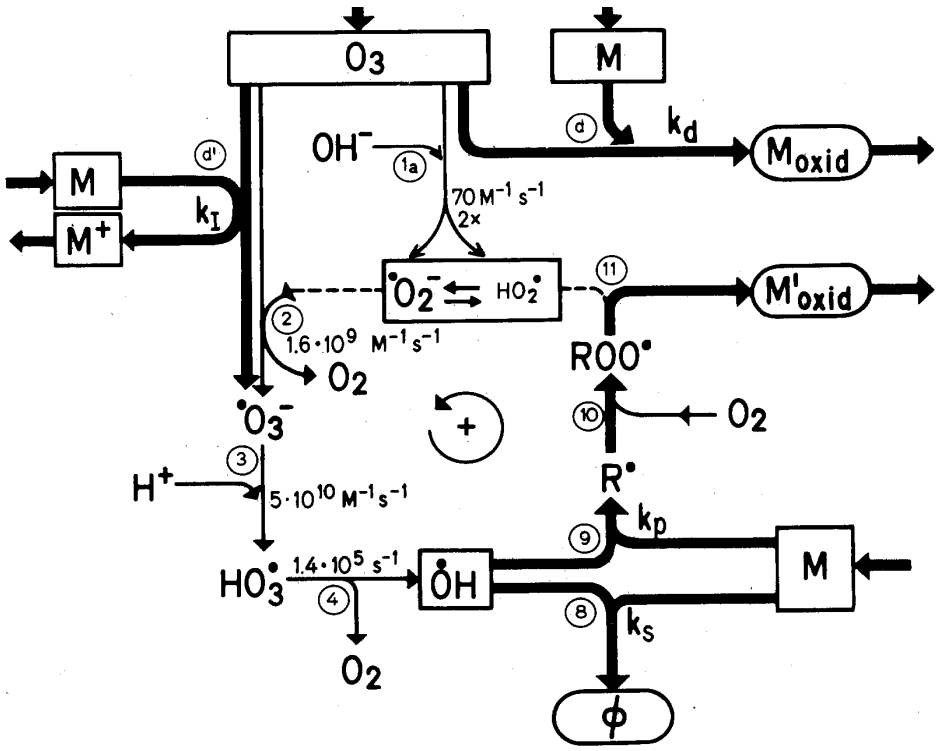

Figure 1.3 Series of reactions described by Hoigne[36], resulting from the degradation of ozone in the presence of solutes M.

spontaneously homolyzes to yield O_2 and HO·. The net stoichiometry of this process is 3 O_3 are consumed per 2 HO· produced. Ozone decomposition is kinetically controlled by OH^- concentration and modeled by:

$$-\frac{d[O_3]}{dt} = k_{O_3,OH^-}[O_3]^1[OH^-]^1 \qquad [52]$$

Equation 53 details the calculation of the theoretical HO· steady state concentration given the concentration of initiators and scavengers in the system:

$$HO\cdot_{ss} = \frac{2k_1[OH^-]+k_I[M]}{k_s[M]}[O_3] \qquad [53]$$

Staehelin and Hoigné[35] also showed the decomposition of ozone could be affected by the addition of hydrogen peroxide through the peroxone reaction:

$$H_2O_2 \rightleftarrows H^+ + HO_2^- \quad \text{pKa-11.6} \qquad [54]$$

$$HO_2^- + O_3 \rightarrow HO_2 \cdot + O_3^- \cdot \quad [55]$$

$$HO_2 \cdot \rightleftarrows O_2^- \cdot + H^+ \quad \text{pKa-4.8} \quad [56]$$

$$O_2^- \cdot + O_3 \rightarrow O_2 + O_3^- \cdot \quad [57]$$

$$O_3^- \cdot + H^+ \rightleftarrows HO_3 \cdot \quad [58]$$

$$HO_3 \cdot \rightarrow HO \cdot + O_2 \quad [59]$$

In this series of reactions, the slow oxygen atom transfer step is augmented by the addition of hydrogen peroxide. O_3 has a much higher rate constant with HO_2^- (5.5×10^6)[35] than with H_2O_2 (0.06)[35]. Staehelin and Hoigne observed that above pH values of 5, O_3 decomposition greatly increased at approximately 1 order of magnitude per pH unit.[36] Given the pKa of H_2O_2 of 11.6, at pH 8 or greater this addition results in significant HOO^- addition, with increased yield of HO·. The net stoichiometry for this process is 2 O_3 consumed per 2 HO· produced. Although the net process is more efficient in terms of ozone utilization, the cost (for drinking water disinfection) of higher efficiency equals the cost of adding food-grade hydrogen peroxide as a reagent. Depression of the steady state concentration of HO· may result from the reaction of HO· with H_2O_2 when increasing amounts of HO· are generated through the peroxone reaction.

Initiators, promotors, and inhibitors of ozone decomposition are commonly found the water supply[37]. Generated from the reaction of ozone with organic compounds, initiators directly react with ozone and include OH^-, HOO^-, $\cdot O_2^-$, and Fe^{II}. Promotors can form $\cdot O_2^-$ from the reaction of HO· and organics, leading to faster O_3 decomposition. These compounds can include formate, O_3, polyalcohols, and sugars. Inhibitors react directly with HO· but do not generate species that contribute to the decomposition of ozone. These species can include HCO_3^-, CO_3^{2-}, and other organics. All these species

contribute to a dynamic system in which their concentration affect the O_3 decomposition and $HO\cdot_{ss}$. Glaze and Kang[38] produced a dynamic model to calculate the HO· steady state concentration if scavengers of HO· other than O_3 are present such as carbonate and bicarbonate:

$$[HO\cdot]_{ss} = \frac{2k_8\left(10^{pH-pKa}\right)[H_2O_2][O_3]}{k_{M,HO\cdot}[M]+(1-S_{per})(k_{15}[HCO_3^-]+k_{14}[CO_3^{2-}])} \quad [60]$$

$$CO_3^{2-} + HO\cdot \rightarrow \cdot CO_3^- + OH^- \quad [61]$$

$$HCO_3^- + HO\cdot \rightarrow \cdot HCO_3 + OH^- \quad [62]$$

Carbonate and bicarbonate are major scavengers of hydroxyl radicals common in natural systems and are capable of severely decreasing the efficiency of an AOP. Carbonate is the better scavenger of HO· with a rate constant of $4.2\text{x}10^8$ M^{-1} s^{-1}, and bicarbonate has a rate constant of $1.5\text{x}10^7$ M^{-1} s^{-1} [36]. At the pH of 7.8, over 99% of carbonate is in the form of bicarbonate and less than 1% is present as carbonate. Phosphate can also compete for HO·, however all species of phosphate have rates $<10^6$ M^{-1} s^{-1}, leading to phosphate often being left out of scavenging calculations. To calculate how much HO· is scavenged by a given species, its concentration must be known along with its rate constant with HO·. In addition, the concentrations and rate constants of other scavengers present in the system is required. Elovitz and von Gunten[39] showed that during an ozonation, the ratio of HO· to O_3 was relatively constant during most of an ozonation. This ratio, R_{ct}, is dependent on water quality and conditions (pH, temperature, etc.), and when determined for a given system, directly correlates to the HO· to O_3 ratio as seen in equation 16.

$$R_{ct} = \frac{[HO\cdot]}{[O_3]} \quad [63]$$

To calculate the fraction (X) of HO· a scavenged by a species (S), the concentration of S times its rate constant with HO· is divided by the sum of all scavengers' times their respective rate constants:

$$X_{HO/S} = \frac{k_{HO/S}[S]}{k_{HO/S}[S]+k_{HO/S_2}[S_2]+\ldots} \quad [64]$$

Due to the limitations of the AOPs (e.g. carbonate scavenging, HO· dismutation, cost of HO· production due to power and reagents, etc.) that reduce their efficiency, modifying these techniques to reduce their deficiencies has been a popular topic of research. Developing a technique that allows the oxidation of certain solution constituents more than others could counter the low efficiencies of the AOPs.

One idea is to introduce an inert solid to heterogenize a process, leading to an increase in the selectivity of organic substrate oxidation. When used in conjunction with ozone, this process is called as heterogeneous ozonation. Different types of solids used to probe the ability of heterogeneous ozonation include metal oxides, activated carbon, and zeolites doped with metals such as titanium. There have been many published examples of heterogeneous catalysts increasing the oxidation rate of organic molecules.[40] Nitrobenzene has been studied thoroughly using multiple different heterogeneous phases as a model organic micropollutant due to its low rate constant with ozone (0.09 M^{-1} s^{-1}) and high rate constant with HO· ($2.2x10^8$ M^{-1} s^{-1}). Yang et al.[41] synthesized a nano-TiO_2 for use as a solid phase during ozonolysis. Above pH of 6, ozonation and heterogeneous ozonation were very similar (no statistical tests were performed), with heterogeneous ozonation providing slightly higher removal rates of nitrobenzene. Below pH 6, heterogeneous ozonation ranged from 3 to 5 times higher removal rates of nitrobenzene. Their data suggested that HO· production accelerated when TiO_2 was added, mostly

occurred in solution, not on the surface of the TiO_2. Ma et al.[42] studied the removal of nitrobenzene during heterogeneous ozonation using granular activated carbon (GAC) and Manganese loaded GAC. It was hypothesized that using manganese, with a high catalytic activity, adsorbed onto GAC, would be effective at adsorbing organics and increasing the rate of ozone decomposition. It was observed that degradation of nitrobenzene increased almost by almost 10% when GAC was added versus ozonation alone. The addition of manganese loaded GAC increased the degradation of nitrobenzene and had an increase of 20-30% versus ozonation alone. Zhang and Ma[43] used a synthetic goethite (FeOOH) to improve the oxidation of nitrobenzene. Due to the presence of adsorbed alkalis on the surface of commercially available goethite which are a by-product of their production, they carefully synthesized the goethite to be as free as possible of alkali so they could best understand the catalytic activity of the goethite and not be interfered with by the pH changes alkali can cause. The combination of ozone and goethite degraded nitrobenzene twice as fast as with ozone alone. Figure 1.4 demonstrates the mechanism of hydroxyl radical generation from the decomposition of ozone on the surface of goethite. Not only was the goethite effective at increasing the degradation of ozone, therefore producing more $HO\cdot$, it appeared to lose very little of its catalytic ability after being reused seven times. This stability would be crucial to the industrial water treatment process to help keep costs manageable by reusing heterogeneous suspensions.

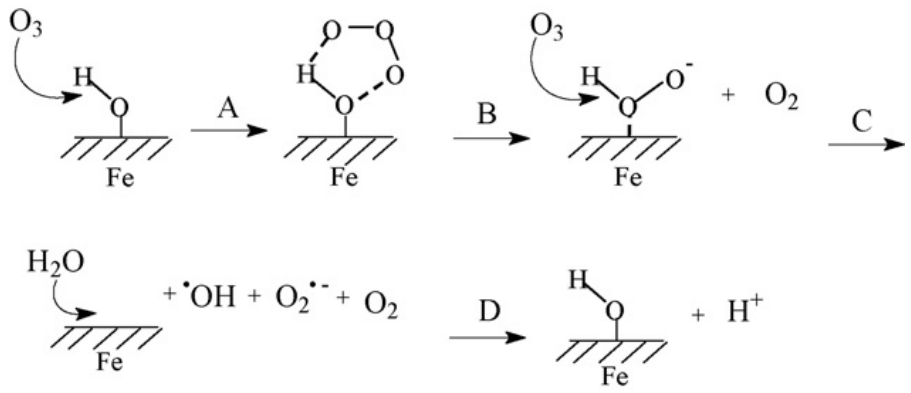

Figure 1.4 Proposed mechanism of hydroxyl radical generation from the reaction of goethite with ozone.[43]

Zeolites are aluminosilicate particles in the same family as molecular sieves that have many uses in industry and research. Zeolites can occur naturally in minerals such as thomsonite or can be artificially synthesized. Among their uses are ion exchange, water purification, sorbents, and petrochemical catalysts during cracking reactions. Zeolites have an ordered structure with channels on the surface that can allow selective adsorption based on size and affinity for the particle. Artificially synthesized zeolites are commercially produced with varying SiO_2/Al_2O_3 ratios, cell sizes, surface areas, and doped metals.[44]

The adsorption of ozone to zeolites has been shown to be influenced by the SiO_2/Al_2O_3 ratio by Fujita et al.[45] ZSM-5 zeolite (SiO_2/Al_2O_3=3000) showed the highest adsorption capacity of ozone compared to silica gel and activated carbon; with a decrease in ozone adsorption correlating with a decrease in SiO_2/Al_2O_3 (SiO_2/Al_2O_3=30, 80, 280, 3000). Ikhlaq et al.[46] concluded that while the ZSM-5 zeolite combined with O_3 was effective in removing an organic probe, it was due to the ability to adsorb both O_3 and the probe and facilitate their reaction on the zeolite; as opposed to decomposing O_3 and removing the organic via radical reactions. Fujita et al.[45] also showed that the

decomposition of ozone in the presence of alumina does result in radical reactions producing ROS. The decomposition resulted from the reaction of O_3 with surface OH^- groups on alumina initiating the decomposition of O_3. This pH dependent process resulted in the greatest amount of ROS being generated when $pH=pH_{PZC}$.

Use of zeolites for catalysis during ozonation is relatively new. Valdes et al.[47] showed that the use of zeolites increased the rate of decomposition of ozone over a pH range of 2-8. They also observed a significant increase in the decomposition rate of ozone when the zeolite was were treated with a 2M HCl-hydroxylamine soak to remove any naturally occurring metal oxides on the zeolite. This was attributed to an increase in Lewis acid sites on the surface of the zeolite through the removal of aluminum and its replacement by 4 hydroxyl groups from water. This agreed with the observation of a decrease in pH_{PZC} from 7.9 to 2.7.

1.3 Experimental Materials

Monosodium phosphate, disodium phosphate, and sodium hydroxide were obtained from Fisher Scientific. 3-nitro-benzotrifluoride (TFNT), dichloroacetic acid (DCAA), and potassium indigotrisulfonate were obtained from Sigma Aldrich. CBV-720 Zeolite was obtained from Zeolyst International. A Zetasizer Nano ZS was used to determine the particle size of the zeolite. 94% of the CBV-720 had a particle size ranging from 0.95-2.3 μm (Figure 1.5), and the suspension had a low dispersity index of 0.35 indicating low uniformity of particle size.

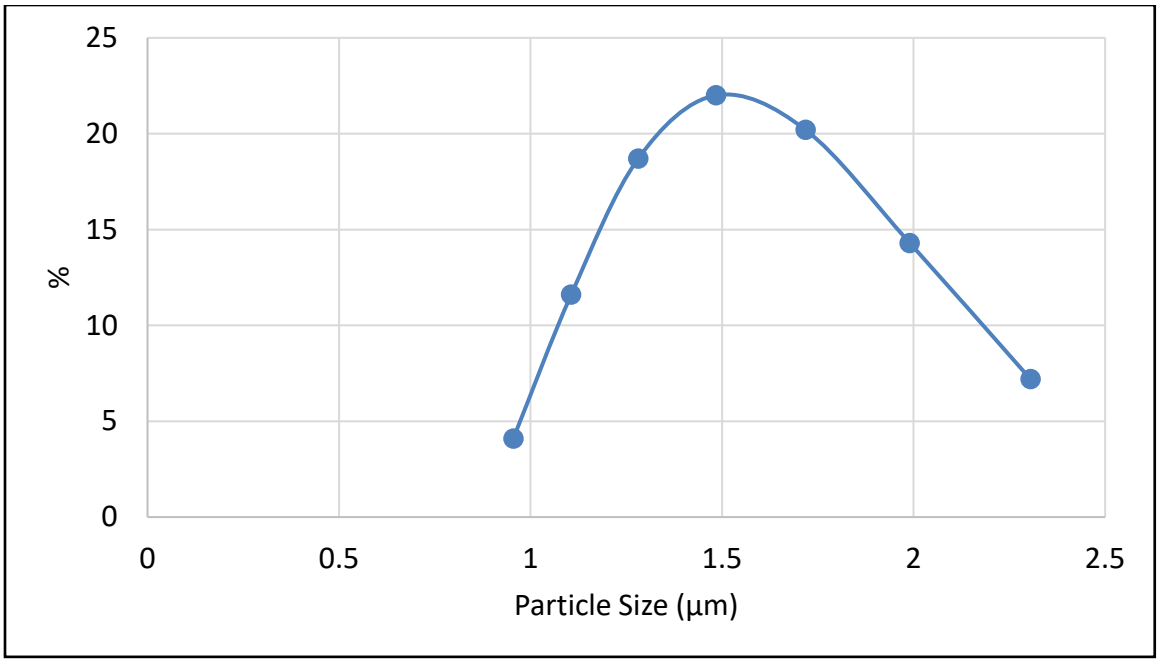

Figure 1.5 Particle size distribution of CBV-720 zeolite

Ozone was produced using a MP-8000 ozone generator from A2Z Ozone Inc, capable of producing 8 g per hour. The generator was fed with an oxygen tank with a set flow rate of 2 L per minute. This flow rate was chosen because it was the lowest recommended flow rate for the generator and allowed for the least amount of air stripping of ozone in the reservoir. Unless otherwise noted, all reagents were used without purification, and all solutions were made with 18 MΩ water. All glassware was soaked overnight in a ~10% HCl and 0.1 M sodium oxalate bath and then cleaned in a muffle furnace.

Procedures

Reactors and Sampling

A 400 mL semi-batch reactor with magnetic stirring was used in all experiments. Ozone saturated water (unbuffered) was siphoned from a 40 L O_3 saturated reservoir into each reactor. Buffer, HO· probes, and zeolite were immediately added to the reactor and a time 0 measurement was taken. Sampling then occurred every 30 seconds for 5 minutes. Triplicate analysis was performed on each reactor condition for statistical power. Each reactor produced two data sets: O_3 vs time and TFNT/DCAA vs time. O_3 was measured spectrophotometrically using potassium indigotrisulfonate (λ_{max}= 600 nm, ε= 20,000 M^{-1} cm^{-1}). Aqueous ozone concentrations typically measured around 100-150 uM. Liquid-liquid extraction using MTBE removed TFNT and DCAA from aqueous solution and diazomethane was added to convert DCAA to its methyl ester for analysis using an HP 6890 GC with a Modular Accelerated Column heater (MACH) and an electron capture detector. The injector port was set for splitless operation at 250 °C. The

autoinjector volume was set at 1 µL. The analytical column was a 15-m DB-5, with a 0.25-µm film thickness. The temperature program was as follows: hold at 60° C for 20s, ramp at 90°/min to 290° and hold for 25s.

1.4 Results

TFNT was used as an HO· probe capable of adsorbing to the zeolite, while being resistant to direct reaction with ozone. No literature values for the oxidation rate of TFNT with O_3 or HO· is available, however similar molecules in structure and composition demonstrate rates with HO· of $1x10^9$-$5x10^9$ (for calculations involving TFNT $k=2.5x10^9$ M^{-1} s^{-1} is used). Ozonation of TFNT at pH ~2.0 confirmed the very slow oxidation rate of TFNT by ozone (Figure 1.6). The lifetime of ozone is inversely proportional to pH, therefore any loss of TFNT at pH 2 is due to the direct reaction of ozone and TFNT. When pH is raised to 7.8 (Figure 1.7), O_3 is decomposed by OH^- and begins the production of HO· to remove TFNT at a rate ~40 times faster than at pH 2 (Figure 1.6). DCAA was chosen as an HO· probe that would not adsorb to the zeolite and be resistant to direct reaction with ozone. Dichloroacetate is unreactive towards ozone with a rate constant of 0.09 M^{-1} s^{-1} and reactive with HO·, $2.3x10^8$ M^{-1} s^{-1} [48]. Dichloroacetic acid has a low pKa of 1.35, therefore at pH 7.8, all DCAA should be in the deprotonated form. Figure 1.8 demonstrates that ozonation at pH 7.8 will produce enough HO· to remove DCAA. At pH 7.8, any loss of DCAA is a result of oxidation by HO·. To ensure the adsorption of TFNT to CBV-730, a Langmuir isotherm showed that TFNT has a strong affinity for the zeolite (Figure 1.9). Adsorption isotherms describe the non-specific

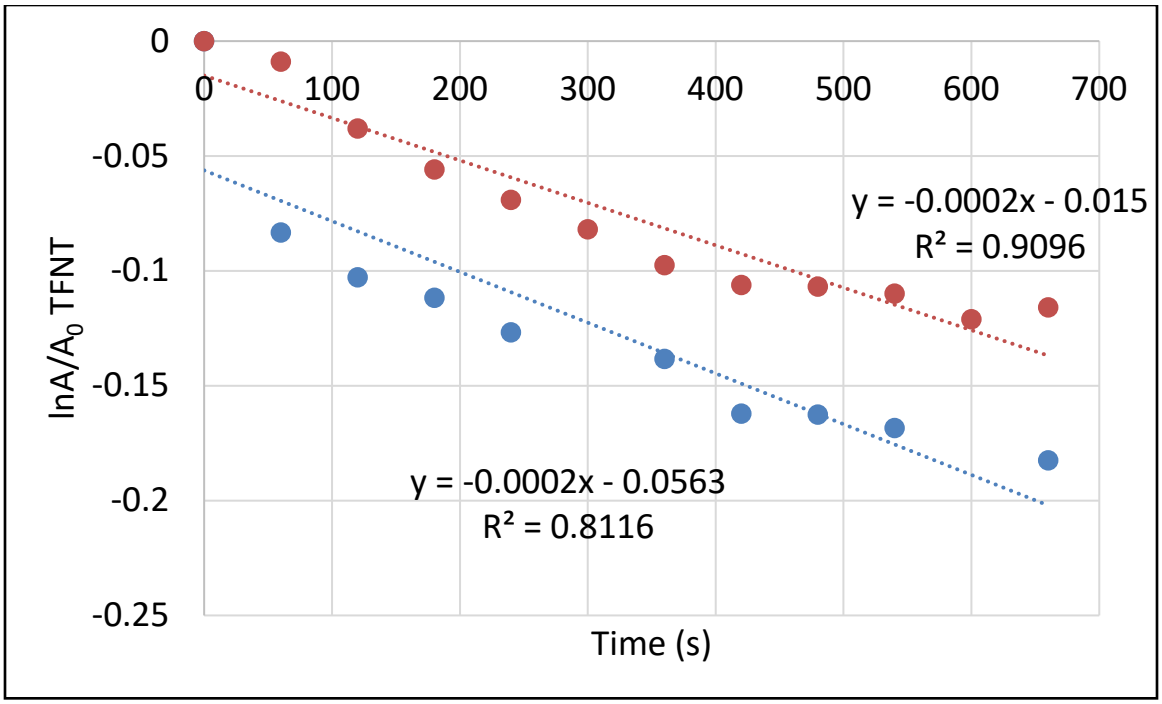

Figure 1.6 Ozonation of TFNT at pH 2.0 using H_2SO_4 was first order over the course of the experiment.

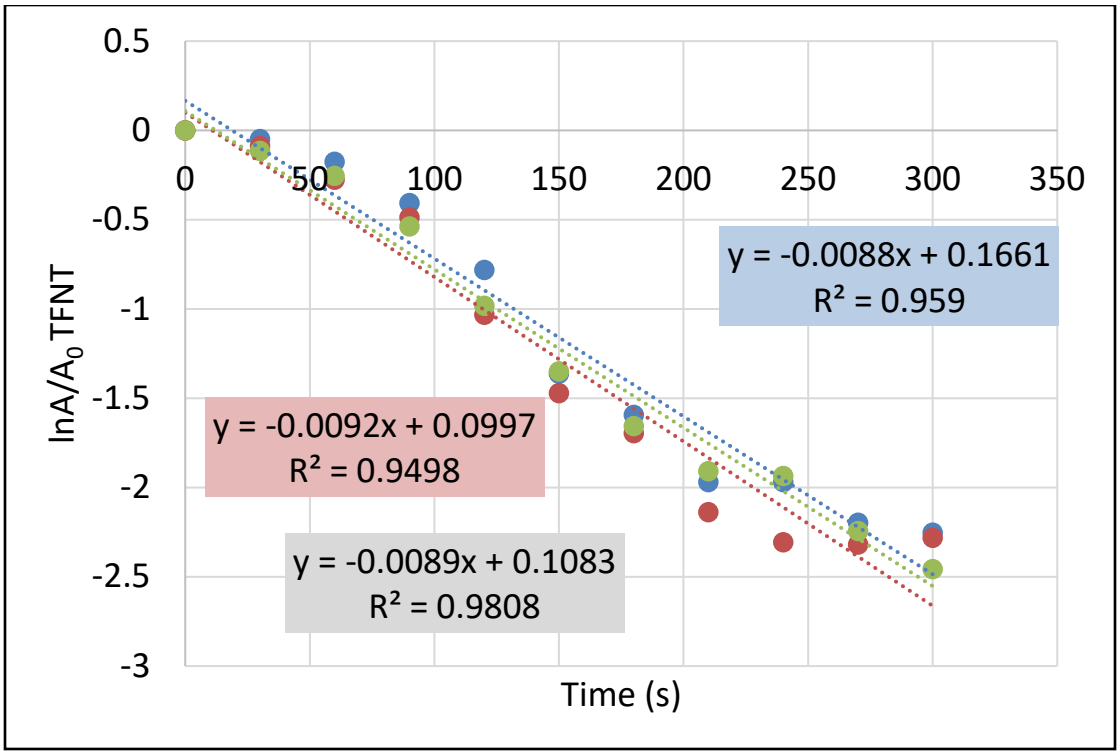

Figure 1.7 Ozonation of TFNT at pH 7.8 with a 12.5 mM phosphate buffer was first order over the course of the experiment.

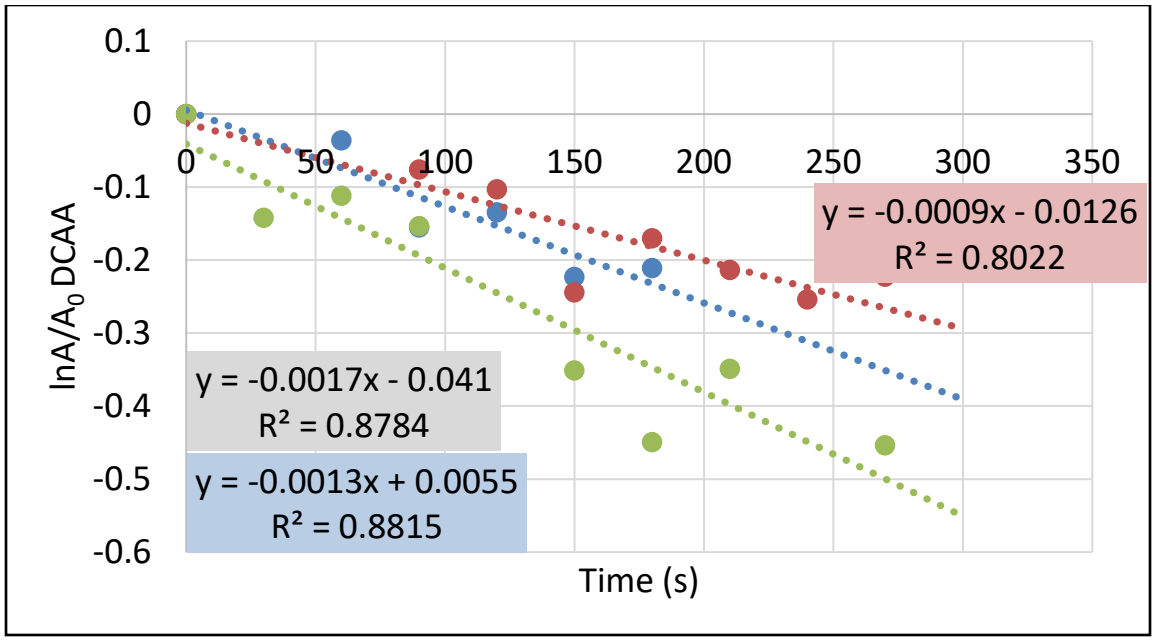

Figure 1.8 Ozonation of DCAA at pH 7.8 with 7mM phosphate buffer was first order over the course of the experiment.

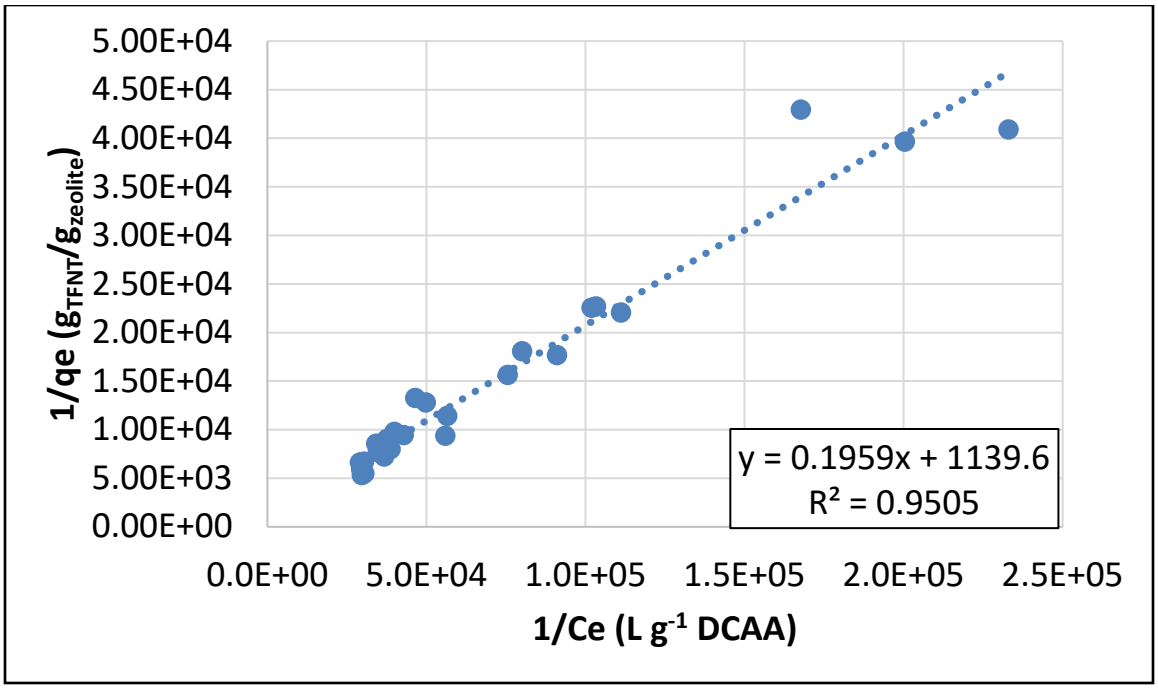

Figure 1.9 Langmuir isotherm demonstrating the strong adsorption of TFNT to CBV-720 when given 24 hours to equilibrate.

binding of an adsorbate to a solid. The Langmuir isotherm assumes a uniform surface and is represented by the equation:

$$q_e = \frac{QbC_e}{1+bC_e} \quad [57]$$

and can be linearized as:

$$\frac{1}{q_e} = \frac{1}{Q} + \frac{1}{QbC_e} \quad [58]$$

Q represents the maximum adsorbate that can be adsorbed onto the surface, and b is the isotherm constant. If b is large and the quantity Qb is much larger than one, the isotherm is considered favorable. Calculating the adsorptive capacity of the zeolite, along with the favorability of the zeolite adsorption of TFNT is done using the linear regression from figure 1.9. Taking the inverse of the slope results in 5.1 being Qb so the adsorption is considered slightly favorable. Calculating the amount of TFNT adsorbed from the inverse of the y-intercept yields 8.775×10^{-4} grams of TFNT per gram of zeolite. Adsorption experiments were performed using dichloroacetic acid which showed negligible amounts of adsorption of DCAA to the zeolite from 0-0.3 wt% (Figure 1.10). The adsorption of TFNT to the zeolite and non-adsorption of DCAA is explained by the presence of an electrical double layer formed on the surface of the zeolite (Figure 1.11). For a negatively charged surface there is a layer of positively charged particles surrounding the surface. After the first layer, there is a second layer of negatively charged particles attracted to the positively charged first layer. DCAA has a pKa of 1.35, therefore at a pH of 7.8, all DCAA is dissociated into the negatively charged dichloroacetate. This should prevent adsorption to the negatively charged zeolite.

Finally, to investigate the rate of adsorption of TFNT to the zeolite, one experiment showing the aqueous concentration of TFNT vs time demonstrated that the TFNT had reached an equilibrium with zeolite in less than one minute.

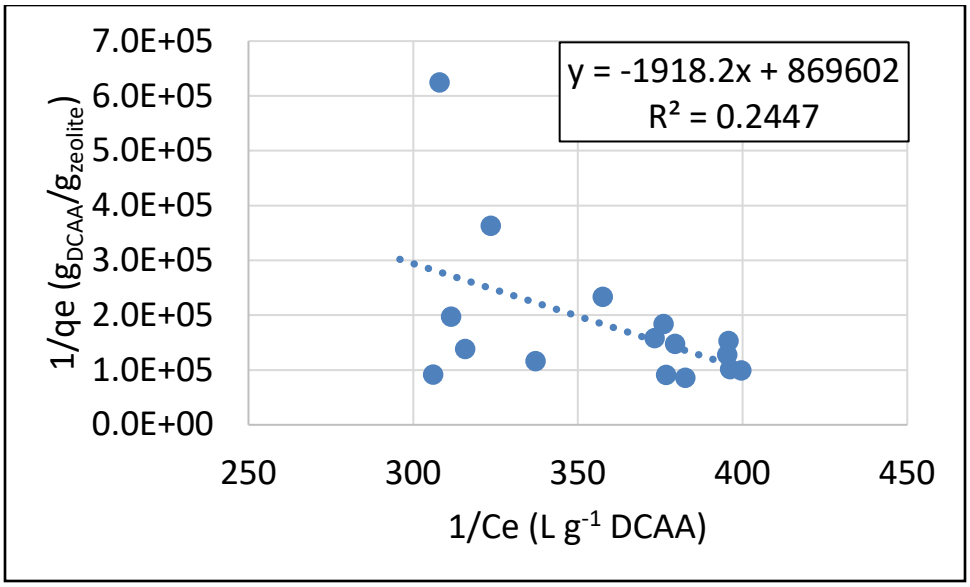

Figure 1.10 Langmuir adsorption isotherm of DCAA to CBV-720 zeolite when given 24 hours to equilibrate. 0.3 wt% zeolite was the highest tested.

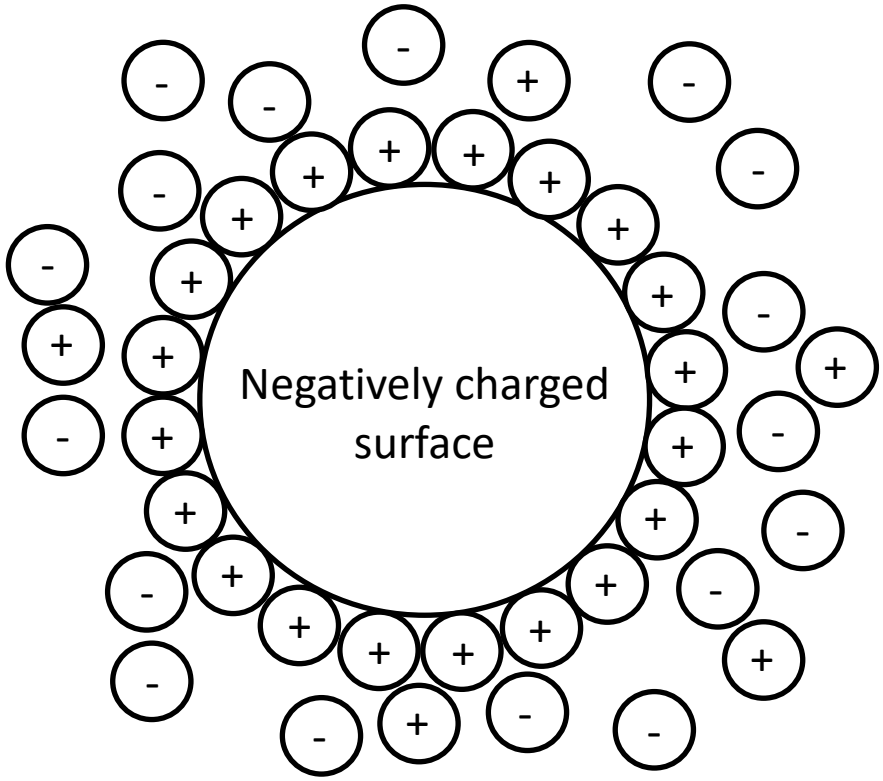

Figure 1.11 An electrical double layer formed on the surface of a negatively charged particle

Zeolite Loading

In the heterogeneous ozonation literature, there is a wide range of concentrations of heterogeneous suspensions used. Investigating different loadings of CBV-720 was essential to understanding if a "sweet spot" existed where the zeolite would act like a promotor of oxidation or if the zeolite consistently suppressed the oxidation rates. The effect on oxidation of TFNT and DCAA over a range of 0-0.2 wt% was studied. Figure 1.12 shows that with increasing amounts of zeolite, oxidation rate of TFNT was significantly lower than when zero zeolite was present, with the exception of 0.05 wt% which was not different at the 95% level of confidence. This agrees with early experiments that used a continuous ozonation reactor where several loadings of zeolite where tested and the fastest oxidation rates were observed in the presence of 0.05 wt% and 0.1 wt%. 0.05 wt% was the chosen zeolite loading used in all experiments using dosed ozonation and from the adsorption experiments. With this concentration of zeolite, ~75% of TFNT added to each reactor is expected to be adsorbed to the zeolite. Looking at the oxidation of DCAA on in figure 1.13, there is no significant difference in the oxidation rate up to 0.2 wt%. This supports the idea that the solution phase chemistry is unaffected by the zeolite, and the chemistry taking place on the surface of the zeolite is being suppressed. Further supporting this idea, figure 1.14 demonstrates the degradation of O_3 over different concentrations of zeolite. There is no significant difference in the loss of O_3 with increasing amounts of zeolite up to 0.2 wt%.

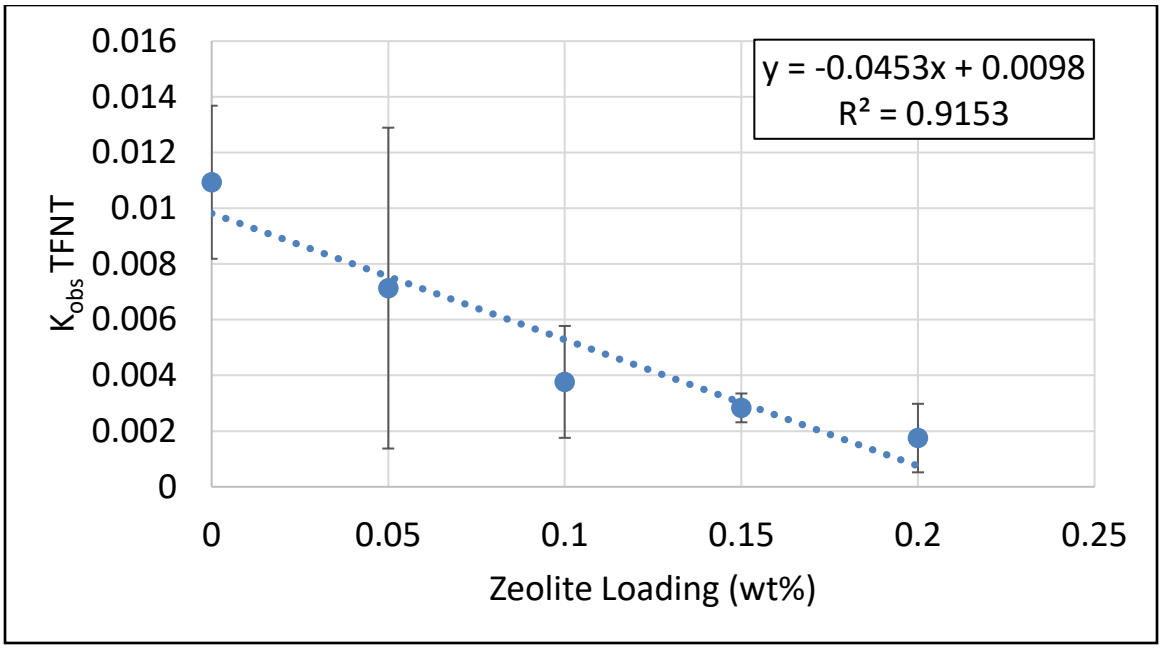

Figure 1.12 The effect of different concentrations of CBV-720 on the oxidation rate of TFNT. (n=3)

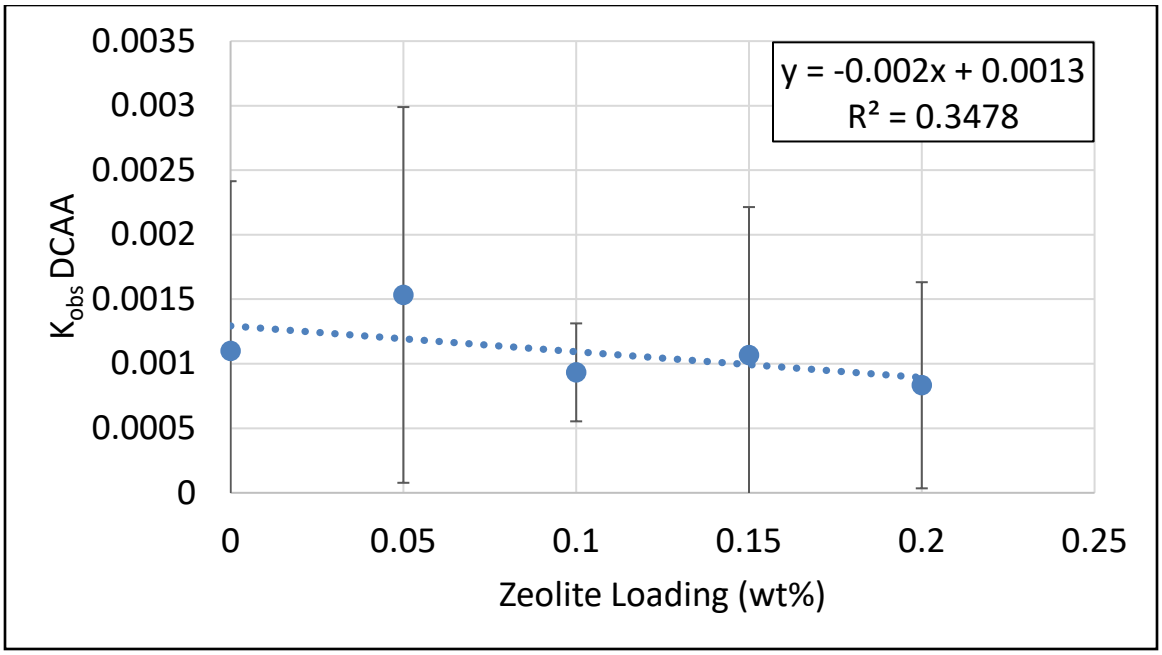

Figure 1.13 The effect of different concentrations of CBV-720 on the oxidation rate of DCAA. (n=3)

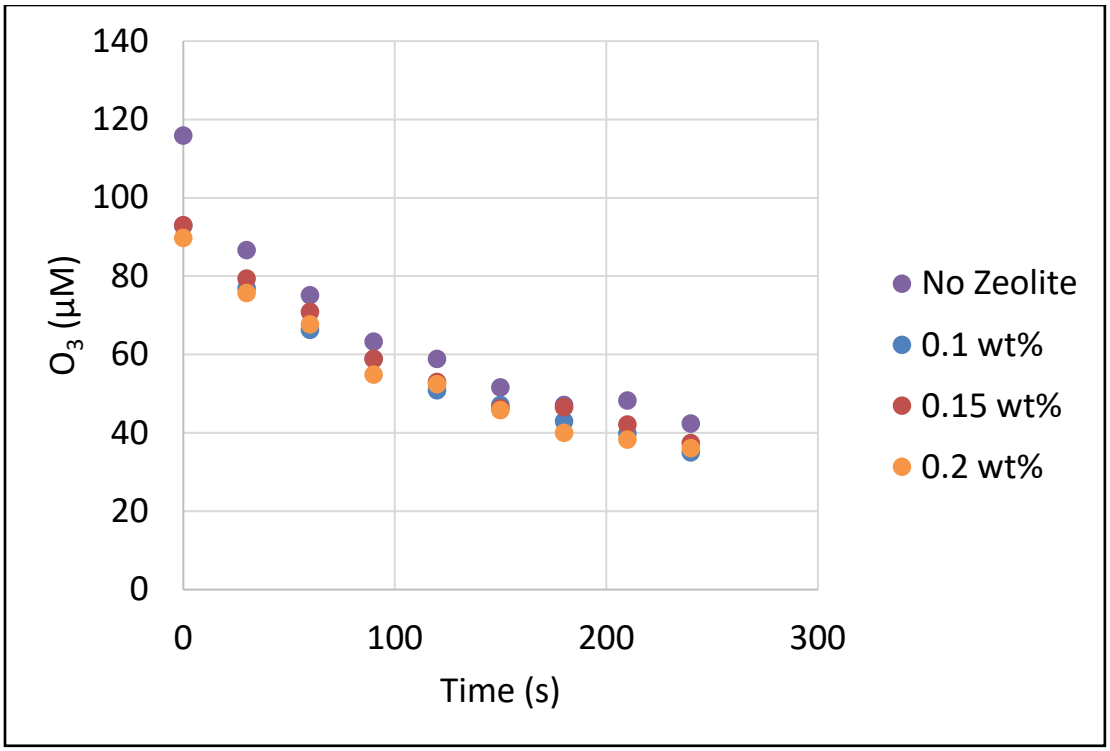

Figure 1.14 The effect of different concentrations of CBV-720 on the degradation rate of ozone

After choosing the 'best' zeolite loading, the effect of a zeolite suspension on ozonation could be investigated. As demonstrated in Figure 1.15, the addition of 0.05 wt% CBV-720 zeolite decreases the oxidation rate of TFNT by ~75%. Later experiments examined the effect of the zeolite on the oxidation of both TFNT and DCAA. Figure 1.16 demonstrates the effect of CBV-720 on the oxidation of TFNT in the presence of DCAA. This results in a decreased oxidation rate of ~50%. The effect of the zeolite on the oxidation of DCAA in the presence of TFNT (Figure 1.16) resulted in an oxidation rate not statistically significant at the 95% confidence interval. We can calculate the ratio of the rate constants and compare it to the observed oxidation rates to help quantify the effect of the zeolite. Assuming equal initial concentrations of DCAA and TFNT, the ratio of the respective rate constants with HO· should be approximately equal to the observed oxidation rates as shown in equation 19:

$$\frac{k_{HO\cdot/TFNT}}{k_{HO\cdot/DCAA}} = \frac{k_{obs,TFNT}}{k_{obs,DCAA}} \quad [59]$$

The ratio of the rate constants of TFNT and DCAA is 10.87 ($2.5x10^9/2.3x10^8$=10.87). Using figures 1.16 and 1.17, the ratio of the oxidation rates with no zeolite comes to 10.9 (0.0109/0.001=10.9). This indicates that HO· is being scavenged by the species is solution as would be expected from theoretical calculations when no zeolite is present. Using the same figures, but using the ratios of the oxidation rates in the presence of 0.05 wt% zeolite, a smaller 4.8 is calculated (0.0072/0.0015=4.8). This shows that HO· is not being scavenged in a way that can be predicted by competitive kinetics.

The difference in the oxidation rate of TFNT and DCAA points to an effect on the surface of the zeolite that inhibits the oxidation of TFNT. No change in the oxidation

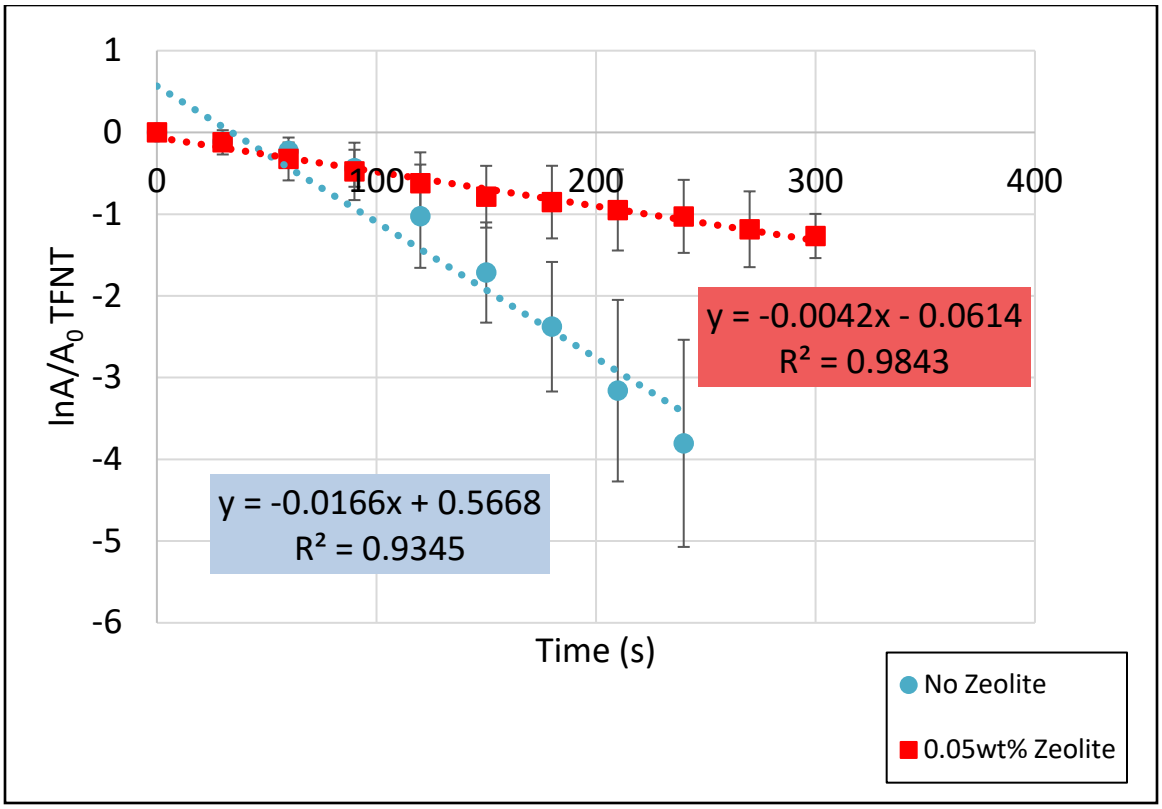

Figure 1.15 The effect of 0.05 wt% CBV-720 zeolite on the ozonation of TFNT. A first order relationship resulted with and without zeolite present. (n=3)

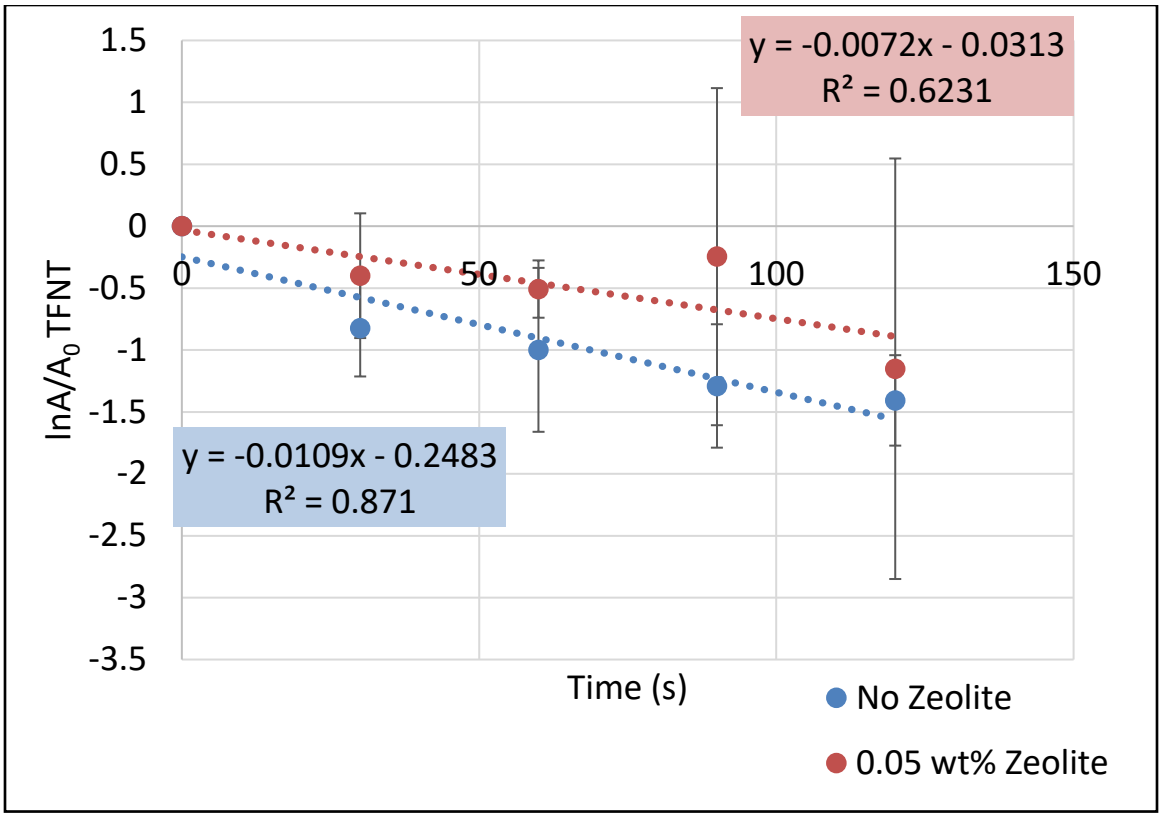

Figure 1.16 The effect of 0.05 wt% CBV-720 zeolite on the ozonation of DCAA in the presence of TFNT resulted in first order relationships. (n=3)

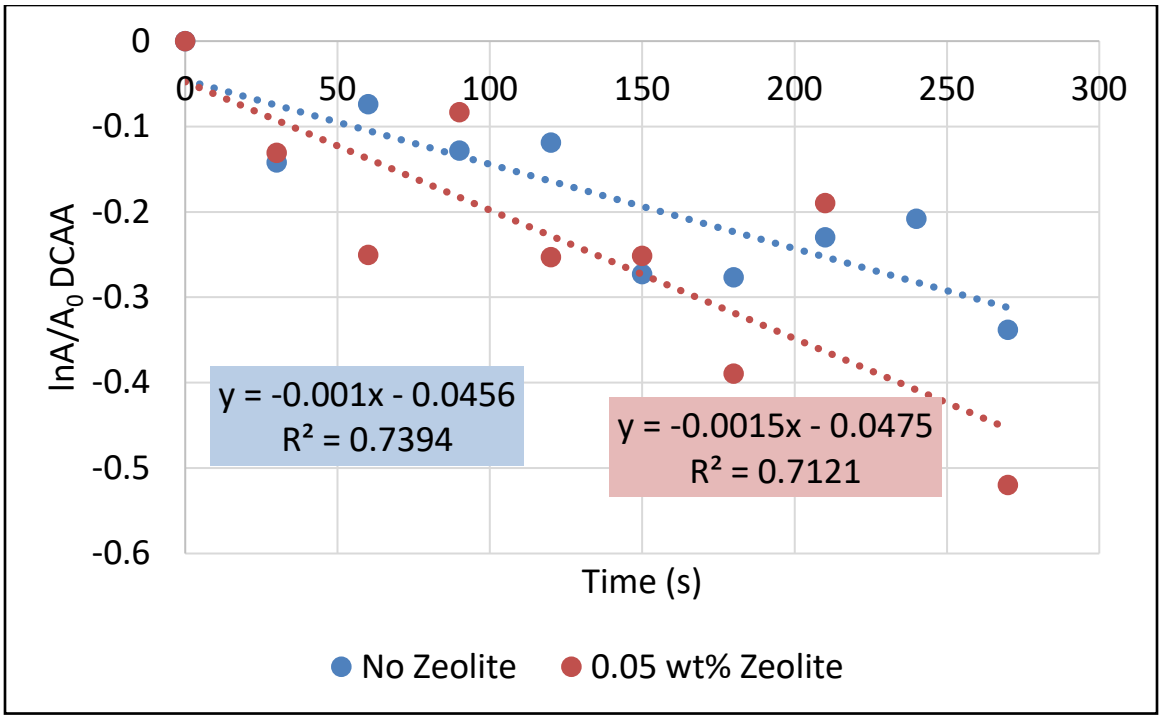

Figure 1.17 Effect of 0.05 wt% CBV-720 zeolite on the ozonation of DCAA in the presence of TFNT resulted in first order relationships. (n=3)

rate of DCAA was observed and it is believed that the zeolite is protecting the TFNT by not allowing HO· to reach TFNT before reacting with other scavengers in solution. Probing the system with one analyte on the surface of the zeolite and another in solution helped gain insight into the fate of HO· through the use of competitive kinetics.

H_2O_2 promoted oxidation

Hydrogen peroxide promotes the degradation of O_3 through the reaction with HO_2^- (equation 47) and increases the $HO\cdot_{ss}$ concentration in solution. Due to the first pKa of H_2O_2 being 11.6, only 0.02% is present as HO_2^- at a pH of 7.8. Despite the low concentration of HO_2^- the addition of H_2O_2 is very effective at degrading ozone. Several experiments were performed in the presence and absence of zeolite with varying amounts of H_2O_2 to investigate the ability of H_2O_2 to accelerate the oxidation of probe molecules enough to overcome the suppression by the zeolite. When 1 μM H_2O_2 is present, the rate of oxidation of TFNT is greatest when no zeolite is present and decreases with an increasing zeolite loading up to 0.2 wt% (Figure 1.18). DCAA is unaffected by the addition of H_2O_2 with increasing zeolite loadings. Substituting the proper terms into equation 45 to calculate $HO\cdot_{ss}$ yields equation 60. From the initial ozone concentration of 150 μM, ~$5.07\text{x}10^{-13}$ M HO· should be expected.

$$[HO\cdot]_{ss} = \frac{2k_1[OH^-]+k_2[HO_2^-]}{k_{HO\cdot/O3}[O_3]+k_{HO\cdot/TFNT}[TFNT]} \quad [60]$$

With the addition of 1 uM H_2O_2, there would be an order of magnitude increase in the HO· concentration, $6.81\text{x}10^{-12}$ M, and it had no effect on the DCAA oxidation. Figure 1.19 shows the comparison between the oxidation rates of TFNT and DCAA when H_2O_2 is present at 1 μM and when there is no H_2O_2 in the system. The addition of H_2O_2

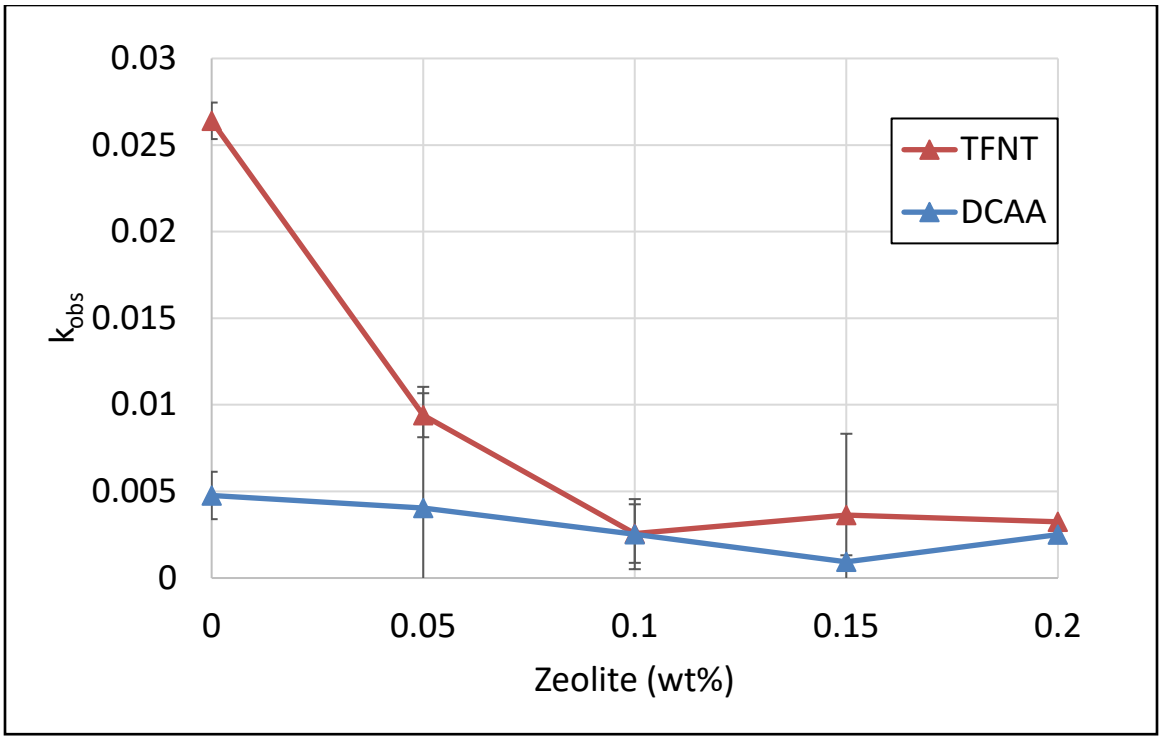

Figure 1.18 The effect of different concentrations of CBV-720 on the oxidation rate of TFNT and DCAA in the presence of 1µM H_2O_2. (n=3)

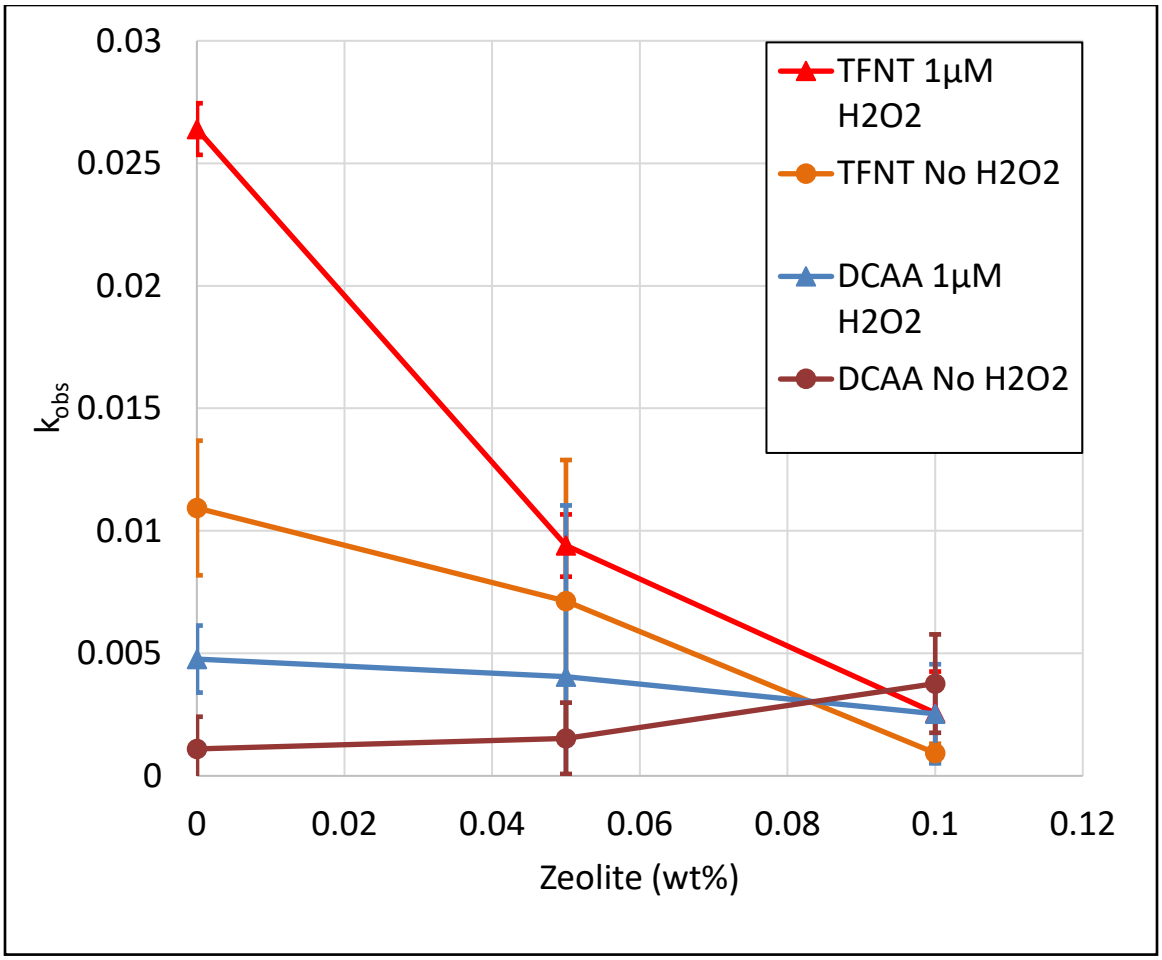

Figure 1.19 The comparison of the effect of H_2O_2 on the oxidation rates of TFNT and DCAA as the loading of zeolite increases. (n=3)

increases oxidation rates but it is not enough to overcome the reduction in oxidation rate by the zeolite.

Bicarbonate HO· Scavenging

Due to the ability of carbonate and bicarbonate to severely reduce the efficiency of AOPs; how zeolites performed in the presence of multiple HO· scavengers were of great interest. If the zeolite is able to facilitate the direct reaction of TFNT and O_3 on the surface of the zeolite and/or allow a greater chance of any HO· generated on or near the surface of the zeolite to react with TFNT instead of being scavenged by HCO_3^- and CO_3^{2-}; it could potentially greatly increase the effectiveness of AOPs in the presence of carbonate HO· scavengers. Figure 1.20 shows that the addition of bicarbonate significantly reduces the oxidation rate of TFNT when 1 mM bicarbonate is present. The zeolite contributes to an almost 90% reduction in oxidation rate under the same conditions. The presence of zeolite has little effect when 3 mM bicarbonate is added, as seen by the convergence of the rates. This is due to only 2.93% of HO· scavenged by TFNT when there is 3 mM bicarbonate alone with no zeolite (Table 1.2). When both zeolite and 3 mM bicarbonate are present, the HO· scavenged by TFNT drops to 0.75%, leaving little HO· to react with TFNT. While the presence of zeolite does not directly affect the HO· scavenging calculation, it does change the aqueous concentration of TFNT. To account for this decrease, the term for the concentration of TFNT is decreased by 75% in the calculation.

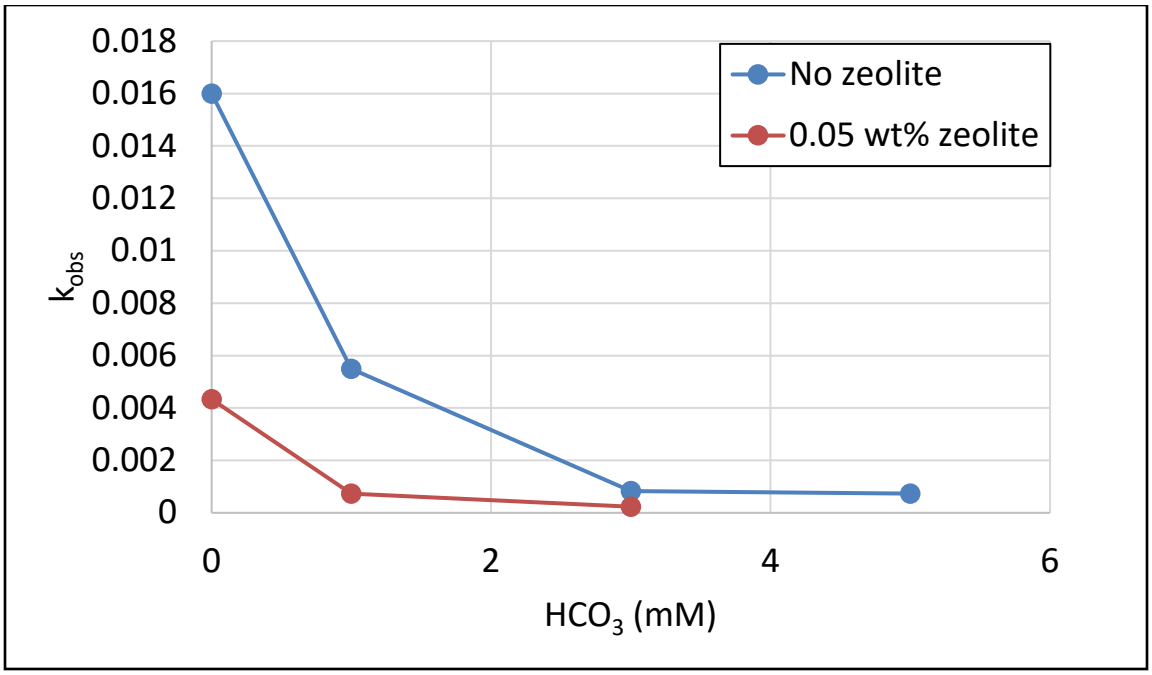

Figure 1.20 The effect of zeolite on the oxidation rate of TFNT when bicarbonate is present as an HO· scavenger. (n=3)

1.5 Conclusions

While the use of heterogeneous ozonation has been shown in the literature to be an effective technology to aid in the removal of contaminants from water, the use of CBV-720 zeolite does not collaborate those findings. This study has found that CBV-720 zeolite only slows down the oxidation of TFNT and has little to no effect on DCAA. It is believed that this is due to the zeolite hindering the access of HO· to molecules that are adsorbed to the surface. If the zeolite sequesters the TFNT and prevents HO· from reaching the TFNT, due to the short lifetime of HO·, reduced amounts of TFNT will be consumed in a system that is ozone limited. While the oxidation of TFNT may have been slowed down, TFNT was still largely removed from solution. Despite being sequestered in an adsorbant, hindering the access of oxidants, contaminants are still susceptible to oxidation from short lived radicals. The significance of this finding can present a challenge to water treatment facilities which may have suspended solids in untreated water. If these suspended solids can adsorb and protect contaminants from added oxidants, then the low efficiency of the AOP could be further reduced. This does not mean that CBV-720 zeolite cannot be useful for water treatment however. CBV-720 was able to remove ~75% of the TFNT from the aqueous phase and did not maintain an equilibrium concentration of TFNT with the bulk solution. The addition of this zeolite may be useful as an adsorbent and then removed prior to the application of oxidants.

Table 1.2 Fraction of HO· scavenged by TFNT, O_3, and HCO^{3-} and the effect of zeolite on scavenging

	No Zeolite (7mM PO_4^{3-} buffer)				0.05 wt% Zeolite (7mM PO_4^{3-} buffer)		
CO_3^{2-} (mM)	X(HO·/TFNT)	X(HO·/O_3)	X(HO·/HCO_3^-)		X(HO·/TFNT)	X(HO·/O_3)	X(HO·/HCO_3^-)
0	8.64%	86.37%	-		2.31%	92.35%	-
1	5.26%	52.56%	34.94%		1.37%	54.72%	36.37%
3	2.93%	29.26%	58.32%		0.75%	29.91%	59.63%

1. Maddocks, A.; Young, R.; Reig, P. Ranking the World's Most Water-Stressed Countries in 2040.
2. E. Blanc, K. S., A. Schlosser, H. Jacoby, A. Gueneau, C. Fant, S. Rausch J. Reilly *Analysis of U.S. Water Resources under Climate Change*; Massachusetts Institute of Technology: Cambridge MA, 2013.
3. Trussell, R. R. *Water Reuse: Potential for Expanding the Nation's Water Supply Through Reuse of Municipal Wastewater*; National Research Council:Committee on the Assessment of Water Reuse as an Approach

for Meeting Future Water Supply Needs: 2012, 2012.
4. Groundwater Use in The United States. https://water.usgs.gov/edu/wugw.html.
5. The Groundwater Foundation. 2018.
6. Effort, C. o. F. O. f. M. i. t. N. s. S. R.; Board, W. S. a. T.; Studies, D. o. E. a. L.; Council, N. R., *Alternatives for Managing the Nation's Complex Contaminated Groundwater Sites*. National Academies Press: Washington DC, 2013.
7. Watts, P. *Tetrachloroethylene*; World Health Organization: 2006.
8. Donatello, S.; Tong, D.; Cheeseman, C. R., Production of technical grade phosphoric acid from incinerator sewage sludge ash (ISSA). *Waste Management* **2010,** *30* (8-9), 1634-1642.
9. Cormier, S. A.; Lomnicki, S.; Backes, W.; Dellinger, B., Origin and health impacts of emissions of toxic by-products and fine particles from combustion and thermal treatment of hazardous wastes and materials. *Environmental Health Perspectives* **2006,** *114* (6), 810-817.
10. Gotz, R.; Lauer, R., Analysis of sources of dioxin contamination in sediments and soils using multivariate statistical methods and neural networks. *Environmental Science & Technology* **2003,** *37* (24), 5559-5565.
11. Pera-Titus, M.; Garcia-Molina, V.; Banos, M. A.; Gimenez, J.; Esplugas, S., Degradation of chlorophenols by means of advanced oxidation processes: a general review. *Applied Catalysis B-Environmental* **2004,** *47* (4), 219-256.
12. Shim, H.; Ryoo, D.; Barbieri, P.; Wood, T. K., Aerobic degradation of mixtures of tetrachloroethylene, trichloroethylene, dichloroethylenes, and vinyl chloride by toluene-o-xylene monooxygenase of Pseudomonas stutzeri OX1. *Applied Microbiology and Biotechnology* **2001,** *56* (1-2), 265-269.
13. Deckard, L. A.; Willis, J. C.; Rivers, D. B., EVIDENCE FOR THE AEROBIC DEGRADATION OF TETRACHLOROETHYLENE BY A BACTERIAL ISOLATE. *Biotechnology Letters* **1994,** *16* (11), 1221-1224.
14. Buxton, G. V.; Greenstock, C. L.; Helman, W. P.; Ross, A. B., Critical Review of Rate Constants for Reactions of Hydrated Electrons, Hydrogen Atoms and Hydroxyl Radicals(.OH/.O-) in Aqueous Solution. *Journal of Physical and Chemical Reference Data* **1988,** *17* (2), 513-886.
15. Schwarz, H. A.; Dodson, R. W., EQUILIBRIUM BETWEEN HYDROXYL RADICALS AND THALLIUM(II) AND THE OXIDATION POTENTIAL OF OH(AQ). *Journal of Physical Chemistry* **1984,** *88* (16), 3643-3647.
16. Buxton, G. V.; Greenstock, C. L.; Helman, W. P.; Ross, A. B., CRITICAL-REVIEW OF RATE CONSTANTS FOR REACTIONS OF HYDRATED ELECTRONS, HYDROGEN-ATOMS AND HYDROXYL RADICALS (.OH/.O-) IN

AQUEOUS-SOLUTION. *Journal of Physical and Chemical Reference Data* **1988,** *17* (2), 513-886.
17. Andreozzi, R.; Caprio, V.; Insola, A.; Marotta, R., Advanced oxidation processes (AOP) for water purification and recovery. *Catalysis Today* **1999,** *53* (1), 51-59.
18. Legrini, O.; Oliveros, E.; Braun, A. M., PHOTOCHEMICAL PROCESSES FOR WATER-TREATMENT. *Chemical Reviews* **1993,** *93* (2), 671-698.
19. Murphy, S. A.; Solomon, B. M.; Meng, S. N.; Copeland, J. M.; Shaw, T. J.; Ferry, J. L., Geochemical Production of Reactive Oxygen Species From Biogeochemically Reduced Fe. *Environmental Science & Technology* **2014,** *48* (7), 3815-3821.
20. Murphy, S. A.; Meng, S.; B.M., S.; Dias, D. M. C.; Shaw, T. J.; Ferry, J. L., Hydrous Ferric Oxides in Sediment Catalyze Formation of Reactive Oxygen Species during Sulfide Oxidation. *Frontiers in Marine Science* **2016,** *in press*.
21. Zoschke, K.; Bornick, H.; Worch, E., Vacuum-UV radiation at 185 nm in water treatment - A review. *Water Research* **2014,** *52*, 131-145.
22. Kutschera, K.; Bornick, H.; Worch, E., Photoinitiated oxidation of geosmin and 2-methylisoborneol by irradiation with 254 nm and 185 nm UV light. *Water Research* **2009,** *43* (8), 2224-2232.
23. Rauf, M. A.; Ashraf, S. S., Radiation induced degradation of dyes-An overview. *Journal of Hazardous Materials* **2009,** *166* (1), 6-16.
24. Baxendale, J. H.; Wilson, J. A., THE PHOTOLYSIS OF HYDROGEN PEROXIDE AT HIGH LIGHT INTENSITIES. *Transactions of the Faraday Society* **1957,** *53* (3), 344-356.
25. Rosenfeldt, E. J.; Linden, K. G., Degradation of endocrine disrupting chemicals bisphenol A, ethinyl estradiol, and estradiol during UV photolysis and advanced oxidation processes. *Environmental Science & Technology* **2004,** *38* (20), 5476-5483.
26. Lundholm, C. E., DDE-induced eggshell thinning in birds: Effects of p,p'-DDE on the calcium and prostaglandin metabolism of the eggshell gland. *Comparative Biochemistry and Physiology C-Toxicology & Pharmacology* **1997,** *118* (2), 113-128.
27. Fenton, H. J. H., LXXIII.-Oxidation of tartaric acid in presence of iron. *Journal of the Chemical Society, Transactions* **1894,** *65* (0), 899-910.
28. Pignatello, J. J., DARK AND PHOTOASSISTED FE3+-CATALYZED DEGRADATION OF CHLOROPHENOXY HERBICIDES BY HYDROGEN-PEROXIDE. *Environmental Science & Technology* **1992,** *26* (5), 944-951.
29. Burns, J. M.; Craig, P. S.; Shaw, T. J.; Ferry, J. L., Short-Term Fe Cycling during Fe(II) Oxidation: Exploring Joint Oxidation and Precipitation with a Combinatorial System. *Environmental Science & Technology* **2011,** *45* (7), 2663-2669.
30. Pignatello, J. J.; Oliveros, E.; MacKay, A., Advanced oxidation processes for organic contaminant destruction based on the Fenton reaction and related chemistry. *Critical Reviews in Environmental Science and Technology* **2006,** *36* (1), 1-84.
31. Koppenol, W. H., THE REDUCTION POTENTIAL OF THE COUPLE O3 O-3.- - CONSEQUENCES FOR MECHANISMS OF OZONE TOXICITY. *Febs Letters* **1982,** *140* (2), 169-172.
32. Stumm, W.; Morgan, J., *Aquatic Chemistry*. 2nd ed. ed.; John Wiley & Sons: New York, 1981.

33. Poyatos, J. M.; Munio, M. M.; Almecija, M. C.; Torres, J. C.; Hontoria, E.; Osorio, F., Advanced Oxidation Processes for Wastewater Treatment: State of the Art. *Water Air and Soil Pollution* **2010,** *205* (1-4), 187-204.
34. Chen, W. S.; Juan, C. N.; Wei, K. M., Decomposition of dinitrotoluene isomers and 2,4,6-trinitrotoluene in spent acid from toluene nitration process by ozonation and photo-ozonation. *Journal of Hazardous Materials* **2007,** *147* (1-2), 97-104.
35. Staehelin, J.; Hoigne, J., DECOMPOSITION OF OZONE IN WATER - RATE OF INITIATION BY HYDROXIDE IONS AND HYDROGEN-PEROXIDE. *Environmental Science & Technology* **1982,** *16* (10), 676-681.
36. Staehelin, J.; Hoigne, J., Decomposition of Ozone in Water - Rate of Initiation by Hydroxide Ions and Hydrogen Peroxide. *Environmental Science & Technology* **1982,** *16* (10), 676-681.
37. Staehelin, J.; Hoigne, J., Decomposition of Ozone in Water in the Presence of Organic Solutes Acting as Promoters and Inhibitors of Radical Chain Reactions. *Environmental Science & Technology* **1985,** *19* (12), 1206-1213.
38. Glaze, W. H.; Kang, J. W., Advanced Oxidation Processes - Description of a Kinetic Model for the Oxidation of Hazardous Materials in Aqueous Media with Ozone and Hydrogen Peroxide in a Semibatch Reactor. *Industrial & Engineering Chemistry Research* **1989,** *28* (11), 1573-1580.
39. Elovitz, M. S.; von Gunten, U., Hydroxyl radical ozone ratios during ozonation processes. I-The R-ct concept. *Ozone-Science & Engineering* **1999,** *21* (3), 239-260.
40. Nawrocki, J.; Kasprzyk-Hordern, B., The efficiency and mechanisms of catalytic ozonation. *Applied Catalysis B-Environmental* **2010,** *99* (1-2), 27-42.
41. Yang, Y. X.; Ma, J.; Qin, Q. D.; Zhai, X. D., Degradation of nitrobenzene by nano-TiO2 catalyzed ozonation. *Journal of Molecular Catalysis a-Chemical* **2007,** *267* (1-2), 41-48.
42. Ma, J.; Sui, M. H.; Chen, Z. L.; Wang, L. N., Degradation of refractory organic pollutants by catalytic ozonation - Activated carbon and Mn-loaded activated carbon as catalysts. *Ozone-Science & Engineering* **2004,** *26* (1), 3-10.
43. Zhang, T.; Ma, J., Catalytic ozonation of trace nitrobenzene in water with synthetic goethite. *Journal of Molecular Catalysis a-Chemical* **2008,** *279* (1), 82-89.
44. International, Z. Our Products. http://www.zeolyst.com/our-products.html.
45. Fujita, H.; Izumi, J.; Sagehashi, M.; Fujii, T.; Sakoda, A., Adsorption and decomposition of water-dissolved ozone on high silica zeolites. *Water Research* **2004,** *38* (1), 159-165.
46. Ikhlaq, A.; Brown, D. R.; Kasprzyk-Hordern, B., Mechanisms of catalytic ozonation: An investigation into superoxide ion radical and hydrogen peroxide formation during catalytic ozonation on alumina and zeolites in water. *Applied Catalysis B-Environmental* **2013,** *129*, 437-449.
47. Valdes, H.; Farfan, V. J.; Manoli, J. A.; Zaror, C. A., Catalytic ozone aqueous decomposition promoted by natural zeolite and volcanic sand. *Journal of Hazardous Materials* **2009,** *165* (1-3), 915-922.
48. Maruthamuthu, P.; Padmaja, S.; Huie, R. E., RATE CONSTANTS FOR SOME REACTIONS OF FREE-RADICALS WITH HALOACETATES IN AQUEOUS-SOLUTION. *International Journal of Chemical Kinetics* **1995,** *27* (6), 605-612.

49. Bader, H.; Hoigne, J., Determination of Ozone in Water by the Indigo Method. *Water Research* **1981,** *15* (4), 449-456.
50. Glaze, W. H.; Kang, J. W.; Chapin, D. H., The Chemistry of Water Treatment Processes Involving Ozone, Hydrogen Peroxide, and Ultraviolet Radiation. *Ozone-Science & Engineering* **1987,** *9* (4), 335-352.
51. Glaze, W. H.; Kang, J. W., Advanced Oxidation Processes for Treating Groundwater Contaminated with TCE and PCE - Laboratory Studies. *Journal American Water Works Association* **1988,** *80* (5), 57-63.
52. Hoigne, J.; Bader, H., Role of Hydroxyl Radical Reactions in Ozonation Processes in Aqueous Solutions. *Water Research* **1976,** *10* (5), 377-386.
53. Hoigne, J.; Bader, H., Rate Constants of Reactions of Ozone with Organic and Inorganic Compounds in Water. 1. Non-Dissociating Organic Compounds. *Water Research* **1983,** *17* (2), 173-183.
54. Hoigne, J.; Bader, H., Rate Constants of Reactions of Ozone with Organic and Inorganic Compounds in Water. 2. Dissociating Organic Compounds. *Water Research* **1983,** *17* (2), 185-194.
55. Glaze, W. H.; Kang, J. W., Advanced Oxidation Processes - Test of a Kinetic Model for the Oxidation of Organic Compounds with Ozone and Hydrogen Peroxide in a Semibatch Reactor. *Industrial & Engineering Chemistry Research* **1989,** *28* (11), 1580-1587.
56. Glaze, W. H.; Lay, Y.; Kang, J. W., Advanced Oxidation Processes- A Kinetic Model for the Oxidation of 1,2-dibromo-3-chloropropane in Water by the Combination of hydrogen peroxide and UV-Radiation. *Industrial & Engineering Chemistry Research* **1995,** *34* (7), 2314-2323.